UNCLASSIFIED
Security Classification

AD737310

DOCUMENT CONTROL DATA - R & D

(Security classification of title, body of abstract and indexing annotation must be entered when the overall report is classified)

1. ORIGINATING ACTIVITY *(Corporate author)*
Denver Research Institute
University of Denver
Denver, CO 80210

2a. REPORT SECURITY CLASSIFICATION
UNCLASSIFIED

2b. GROUP

3. REPORT TITLE

THE AGING RESPONSE OF SHOCK DEFORMED NICKEL-BASE SUPERALLOYS

4. DESCRIPTIVE NOTES *(Type of report and inclusive dates)*
Final Report, 5 Nov. 1970 - 5 Dec. 1971

5. AUTHOR(S) *(First name, middle initial, last name)*
R. Norman Orava

6. REPORT DATE	7a. TOTAL NO. OF PAGES	7b. NO. OF REFS
January 1972	58	50

8a. CONTRACT OR GRANT NO.	9a. ORIGINATOR'S REPORT NUMBER(S)
NOOO19-71-C-0099	DRI #2592
b. PROJECT NO.	
c.	9b. OTHER REPORT NO(S) *(Any other numbers that may be assigned this report)*
d.	

10. DISTRIBUTION STATEMENT
Distribution of this document is unlimited.

RELEASED TO PUBLIC PER SEC DEF MEMO TO SEC NAV 29 May 1969 under 6.1 category funding program

11. SUPPLEMENTARY NOTES

12. SPONSORING MILITARY ACTIVITY
Naval Air Systems Command
Washington, D.C. 20360
Attn: Code AIR-52031B

13. ABSTRACT

An investigation was conducted to study the effect of explosive shock loading on the microstructure and mechanical properties of subsequently age-hardened Udimet 700 nickel-base superalloy. Such shock thermomechanical processing (TMP) has been termed shock-aging. The results of shock TMP, conventional TMP by cold rolling, and thermal processing alone, were compared. U-700 sheet was subjected to a planar plastic shock wave, or rolled to a strain equivalent to the transient shock strain, in each of three initial conditions: solution treated, (γ') aged, or carbide aged. The highest shock pressure examined was 527 kbar, with a corresponding reduction in thickness by rolling of 19.1%. Substantial improvements in strength at room temperature and 1200 F were effected by both conventional and shock TMP. However, the former (19.1% reduction) lowered tensile ductility at 1200 F whereas it was shown that shock-aging (527 kbar pressure) could lead to ductility increases of 200 to 400% depending on the heat treatment parameters. Shock TMP produced increases in stress-rupture life at 1200 F as high as 50-fold. A number of microstructural differences, and small dimensional changes (2% at 527 kbar) also favored shock TMP over conventional TMP. About 50% of the observed TMP strengthening was ascribed tentatively to substructure hardening; the remainder was postulated to be due to a fine matrix $M_{23}C_6$ precipitate nucleated at dislocations.

DD FORM 1 NOV 65 1473 (PAGE 1)
S/N 0101-807-6801

Unclassified
Security Classification

14 KEY WORDS	LINK A		LINK B		LINK C	
	ROLE	WT	ROLE	WT	ROLE	WT
Ni-base superalloys Udimet 700 Thermomechanical processing Shock deformation						

DRI No. 2592

THE AGING RESPONSE OF SHOCK DEFORMED NICKEL-BASE SUPERALLOYS

Final Technical Report

Contract No. N00019-71-C-0099
5 November 1970 - 5 December 1971

- Prepared for -

Air Systems Command
Department of the Navy
Washington, DC 20360

- Submitted by -

University of Denver
Denver Research Institute

January 1972

APPROVED FOR THE
DIRECTOR BY

Charles E. Lundin

Charles E. Lundin, Acting
Head, Metallurgy and
Materials Science Division

PREPARED BY:

R. Norman Orava

R. Norman Orava
Research Metallurgist

ABSTRACT

An investigation was conducted to study the effect of explosive shock loading on the microstructure and mechanical properties of subsequently aged Udimet 700 nickel-base superalloy. Such shock thermomechanical processing (TMP) has been termed shock-aging. The results of shock TMP, conventional TMP by cold rolling, and thermal processing alone, were compared. Udimet 700 sheet was subjected to a planar plastic shock wave, or rolled to a strain equivalent to the transient shock strain, in each of three initial conditions: solution treated, γ' aged, or carbide aged. The highest shock pressure examined was 527 kbar, with a corresponding reduction in thickness by rolling of 19.1%. Substantial improvements in strength at room temperature and 1200°F were effected by both conventional and shock TMP. However, the former (19.1% reduction) lowered tensile ductility at 1200°F whereas it was shown that shock-aging (527 kbar pressure) could lead to ductility increases of 200 to 400% depending on the heat treatment parameters. Shock TMP produced increases in stress-rupture life at 1200°F as high as 50-fold. A number of microstructural differences, and small dimensional changes (2% at 527 kbar) also favored shock TMP over conventional TMP. About 50% of the observed TMP strengthening was ascribed tentatively to substructure hardening the remainder was postulated to be due to a fine matrix $M_{23}C_6$ precipitate nucleated at dislocations.

TABLE OF CONTENTS

TABLE OF CONTENTS

LIST OF TABLES

LIST OF TABLES (Concluded)

LIST OF FIGURES

LIST OF FIGURES (Concluded)

1. INTRODUCTION

The gas turbine engine is an outstanding present-day example of an application which challenges the metallurgist to the limit of his ingenuity. This and other demands which are being placed on metallic materials dictate a continuing search for new and improved means of extending their strength and service temperature range. On the one hand, it is difficult to conceive of novel techniques or mechanisms of alloy hardening which are fundamentally different from those already known to be effective. On the other hand, the full utilization of known strengthening methods coupled with processing innovations could conceivably lead to significant improvements in mechanical properties and thermal stability.

One of the outgrowths of high-temperature alloy research was the introduction of nickel-base superalloys[1]. Recently, moreover, there have been a number of important advancements in the field of processing and fabrication of these alloys which are technologically significant. These include the utilization of powder metallurgy techniques to produce large nickel-base alloy components[2-5]. Thereby, the segregation which is a characteristic casting problem with such complex alloys can be circumvented. As a result of the fine grain sizes achievable by powder metallurgy, the compact can exhibit superplastic behavior in a certain temperature and strain-rate range, a phenomenon which can be used to advantage during hot working.

Another processing advancement is directional solidification, designed to produce columnar-grained microstructures[6], single crystals[7,8], or oriented eutectic structures of the composite type[9].

The last few years have also seen the introduction and application of thermomechanical processing (TMP) to high-temperature alloys. This involves the utilization of specific combinations of thermal and mechanical processing treatments in order to effect certain property improvements.

The purpose of the investigation described herein is to evaluate and understand the effect of explosive shock loading prior to aging on the microstructure and mechanical properties of aged nickel-base superalloys. The ultimate goal of the overall program is the improvement of the service capability of this group of alloys. Thus, while TMP forms the basis of the study, there is one major departure from

conventional procedures -- the deformation during mechanical working is imparted at a very high energy rate and more specifically, by the propagation of a plastic shock wave through the material. For convenience, the process has been termed "shock-aging."

The approach is relatively straightforward. Udimet 700, selected for the initial studies, was solution treated, or solution treated and partially aged, shock loaded, and then subjected to one or more additional aging treatments. The room temperature hardness, elevated temperature short-term tensile properties, and stress-rupture life and ductility were determined. These observations were correlated with microstructure as determined by optical and electron metallography. The data were compared with results for Udimet 700 which was thermally processed only, and also, with material which had undergone conventional TMP by cold rolling.

2. THERMOMECHANICAL PROCESSING

Compared with ferrous alloys, the TMP of nickel-base superalloys is necessarily more limited in scope and applicability. Nevertheless, it has been demonstrated convincingly that significant property improvements can be achieved by hot, warm, or cold TMP, or combinations thereof. Since the emphasis in this program is on ambient temperature mechanical working, this discussion is confined mainly to the effects of cold TMP.

Due to their age hardenability, modifications of the processing schedules normally focus on methods of redistributing, dispersing, and refining the precipitates to enhance low and high temperature behavior. Often, one is achieved at the expense of the other. Certain alloys, such as Inconel 718[10] and Monel K-500[11], can be obtained commercially in a condition arrived at by cold working prior to aging (cold-finished). From a 1966 review of the properties of selected superalloys[12], it could be deduced that cold forming Inconel 718, Rene 41, Waspaloy, Monel K-500, and Inconel X-750 prior to aging generally results in an increase in the short-term cryogenic, room, and elevated temperature yield and tensile strengths, with the anticipated decrease in ductility. The corresponding effect on elevated temperature long-term properties is beneficial only at the lower temperature ranges. For example, cold working Inconel 718 prior to aging results in the improvement of the 1000-hour rupture stress at 800°F, but deterioration at 1000°F and higher. Results with hot or warm working during TMP have been equally disappointing[13-17] until recently[18]. Kear et al.[18] illustrated the distinct advantages to both yield and rupture life of a TMP schedule for Udimet 700 which entailed warm working at 1950°F. Moreover, they concluded from the results of a literature survey of the TMP of nickel-base superalloys, and their own observations, that the full potential of TMP in the fabrication of superalloy parts with improved mechanical properties for application at intermediate temperatures could be realized by combining hot and warm working in a TMP schedule. The essential details of this treatment involves hot working just below the γ' solvus temperature to refine the grain size, and then warm working in the superplastic range, a procedure patented by Pratt and Whitney as "GATORIZING."

It is all the more noteworthy then that Blankenship was able to achieve both short- and long-term strength enhancement through the TMP of Udimet 700 utilizing a cold-working process[19, 20]. Hydrostatic

extrusion, followed by aging, resulted in an increase in yield strength at 1000 and 1200°F of as much as 100,000 psi over conventionally heat treated stock. Correspondingly, the stress rupture life at 1200°F was raised from 400 to over 3700 hours -- nearly an order of magnitude improvement. The increases are less pronounced at a testing temperature of 1400°F depending on the amount of prior strain, but nevertheless substantial. Beyond this temperature, however, the difference in the behavior between thermomechanically processed and thermally processed materials are expected to diminish rapidly.

Little attempt was made in the preceding investigation to correlate the observed properties with microstructure, or to interpret the findings. A number of explanations are possible. It is believed by most that the small coherency strain of the γ' Ni_3(Al, Ti) precipitate normally precludes its nucleation on dislocations[13, 21]. Conversely, since there is evidence[22] that dislocations can indeed act as nucleation sites for γ', this interpretation cannot be discounted completely. However, it should be kept in mind that solution treated Udimet 700 has a fine γ' precipitate which is formed during the air cool. Accordingly, the effect of a deformation substructure produced after solution treatment on the distribution and morphology of γ' is not expected to be appreciable. The two more attractive possibilities are substructure strengthening[18] and precipitation of carbides ($M_{23}C_6$) on dislocations[23-25].

3. CHARACTERISTICS OF SHOCK-WAVE DEFORMATION

It is reasonable to inquire what unique features can be ascribed to shock deformation that renders it an attractive substitute for more conventional deformation in strain aging or TMP treatments. There are three main characteristics which are important in this respect.

Firstly, a large transient plastic strain is developed with little accompanying permanent dimensional change, i.e., a small residual strain. This results from the fact that irreversible plastic work is done at the compressive shock front, and a nearly equivalent amount is done by the following rarefaction wave. However, the sign is reversed resulting in a net strain of almost zero. The true transient strain is given, in effective or generalized form, as[26]

$$\epsilon_T = 4/3 \ln V/V_0 \qquad (1)$$

where V_0 and V are the initial and compressed volumes, respectively. The ratio V/V_0 can be determined from the Hugoniot-Rankine conservation relations.

A second feature which distinguishes shock-loaded material from its more slowly strained counterpart is one which is a consequence of the high strain rates (10^6 - 10^8 sec^{-1}) developed at the shock front[27]. The requirement to accommodate, in times of the order of 10^{-9} sec, appreciable transient plastic strains dictates that many dislocations move short distances. This normally leads to a higher dislocation density than an equivalent amount of quasi-static flow. Furthermore, the distribution is finer and more uniform[28, 29].

Lastly, Weertman[30] predicted that the efficiency of point-defect generation by dislocations increases with increasing dislocation velocity. This suggestion was confirmed experimentally by Kressel and Brown[31] who examined the resistivity recovery of shocked nickel. They found that the vacancy concentration exceeded the interstitial concentration by an order of magnitude. Also, for equivalent values of plastic strain, the point-defect concentration following shock deformation was appreciably higher than after cold rolling. More recent studies of point-defect clustering in shocked aluminum[32], and the resistivity recovery of Fe-Mn alloys[33] have further substantiated the existence of an extraordinarily high nonequilibrium vacancy concentration in shocked metals.

The enhanced point-defect generation is thought to be the result of the necessity of moving dislocation jogs nonconservatively due to the impedance, at high dislocation velocities, of other mechanisms such as conservative jog motion and cross slip. This process is compounded by the occurrence of a greater number of jog-producing intersections of primary and secondary dislocations during shocking than during lower-rate deformation.

Accordingly, when one is considering strain-enhanced precipitation hardening, shock deformation offers the advantages of small residual strains, a high density of uniformly distributed nucleation sites or pinning points, and the means for accelerating aging.

4. EXPERIMENTAL DETAILS

4.1 Material and Heat Treatment

The selection of Udimet 700* as the nickel-base superalloy to be investigated was dictated by its popularity as a commercial turbine alloy, the encouraging results of conventional cold TMP, and the fact that it was soon to become available in sheet form. The last factor was considered important to future explosive forming and bonding studies.

The Udimet 700 was supplied by the Stellite Division of Cabot Corporation in the form of 0.095-in. thick hot-rolled sheet. Details of its fabrication to sheet of thickness 0.030 and 0.015 in. have been reported by Kelley[34,35]. The chemical analysis in weight percent was given by the supplier as follows:

Element	Stellite U-700 Sheet	Nominal[36]
Al	4.45	3.75 - 5.00
B	0.025	0.01 - 0.05 max.
C	0.10	0.15 max.
Co	14.4	14.00 - 20.00
Cr	15.8	13.00 - 17.00
Mo	4.7	4.50 - 6.00
Ti	3.5	2.75 - 4.00
Fe	--	4.00 max.
Ni	Bal.	Bal.

The cobalt content of the sheet was on the low side of nominal, while the aluminum content was slightly high. The supplier stated that both factors tended to raise the γ' solvus temperature, and estimated it to be about 2085° to 2100°F. Quenching experiments during the course of the present investigation disclosed the complete dissolution of γ' after 30 min. at 2150°F but not at 2100°F. It should be noted, however, that the sheet composition is within the nominal limits quoted by Special Metals, Inc., as demonstrated in the above table.

* Udimet 700 is a registered trademark of Special Metals, Inc.

Accordingly, the following standard heat treatment schedule was adopted[36]:

Solution Treatment (ST)	2150°F, 4 hr, AC
Gamma Prime Age (γ')	1975°F, 4 hr, AC
Carbide Age (C)	1550°F, 24 hr, AC
Final Age (F)	1400°F, 16 hr, AC

The designations in brackets for the different steps will be used throughout the report. Solution treatment and γ' aging were performed in an inert argon atmosphere. The last two aging anneals were conducted in still air.

The phases normally found in fully heat treated wrought Udimet 700 sheet are MC, $M_{23}C_6$, M_3B_2, γ', and a γ matrix[37]. The γ' in the matrix ordinarily appears in two forms -- a cuboidal type, approximately 0.5 μ square, oriented along crystallographic planes. The second form is extremely fine, spheroidal, less than 0.1 μ in diameter, and develops primarily during air cooling and the final aging treatment. Irregularly-shaped, blocky γ' usually envelops the grain-boundary carbides and matrix carbides and borides. The high creep resistance of this group of alloys is attributable in large part to the presence of a $M_{23}C_6$ carbide phase at the grain boundaries. At the same time, the γ' envelope inhibits short-term intergranular embrittlement.

Typical microstructures of the fully heat treated Stellite Udimet 700 sheet are shown in Figure 1. Routine metallographic procedures were followed. Microstructural features were revealed by chemical etching with a solution containing 30 parts lactic acid, 20 parts HCl, and 10 parts HNO_3, and deformation markings by electolytic etching in a solution of 400 parts H_2O, 3 parts HCl. and 1 part HNO_3. Two-stage carbon replicas, shadowed at 45° with platinum-carbon, were examined in a Philips EM200 electron microscope.

4.2 Thermomechanical Processing Schedules

As illustrated in Table 1, deformation was imparted by shock loading or cold rolling the material in each of three initial conditions: solution treated; solution treated and γ' aged; solution treated, γ' and

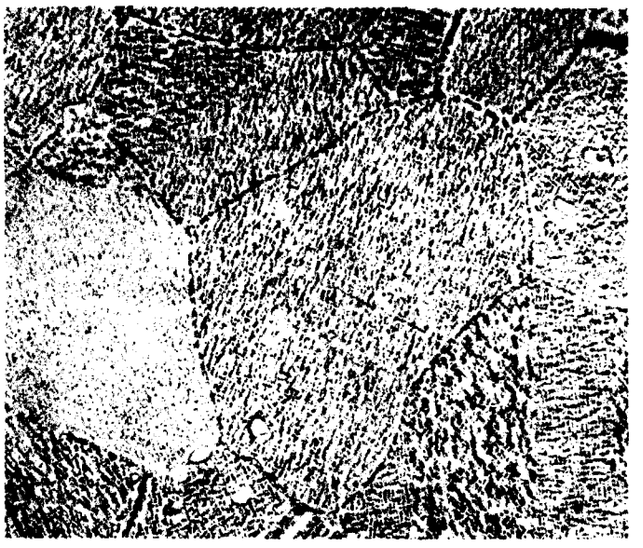

a. Optical; 800X

b. Surface Replica

Figure 1. Microstructure of Fully Heat Treated Stellite Udimet 700 Sheet.

carbide aged. Various aging sequences were applied after mechanical processing. The designations for each schedule can be derived by consideration of Table 1. The hyphen between a letter and number is to be replaced by the correct deformation code. For example, a specimen which was solution treated, cold-rolled, and then given carbide and final aging treatments, can be described as AR6. Its shocked and undeformed counterparts are AS6 and AU6, respectively. Similarly, a sample which has undergone solution treatment, γ' and carbide aging, cold rolling, and then final aging, is characterized as CR7, with CS7 and CU7 pertaining to shock-aged and thermally-processed material, respectively. It is noteworthy that AR6 and CR7 correspond to the two schedules investigated by Blankenship and Gyorgak[19,20]. There is some duplication of schedules for undeformed control material. This is demonstrated by the fact that AU4 = BU6 = CU7, where all of these will be classified simply as STA, the fully heat treated condition.

Table 1. Thermomechanical Processing Schedules for Udimte 700

STA	Schedule A							Schedule B			Schedule C
ST	ST							ST			ST
	Strain*: R or S							---			---
	A-1	A-2	A-3	A-4	A-5	A-6	A-7				
γ'	γ'	γ'	γ'	γ'	---	---	---	γ'			γ'
								Strain: R or S			
								B-5	B-6	B-7	
C	---	C	---	C	C	C	---	C	C	---	C
											Strain: R or S
											C-7
F	---	---	F	F	---	F	F	---	F	F	F

* R = cold-rolled; S = shock-loaded; each schedule includes a "U" code for the undeformed control material.

4.3 Shock-Loading Procedure

Shock deformation was achieved by the propagation through the material of a planar shock wave produced by means of a "mousetrap" generator, illustrated in Figure 2. This accelerates a flyer plate to a

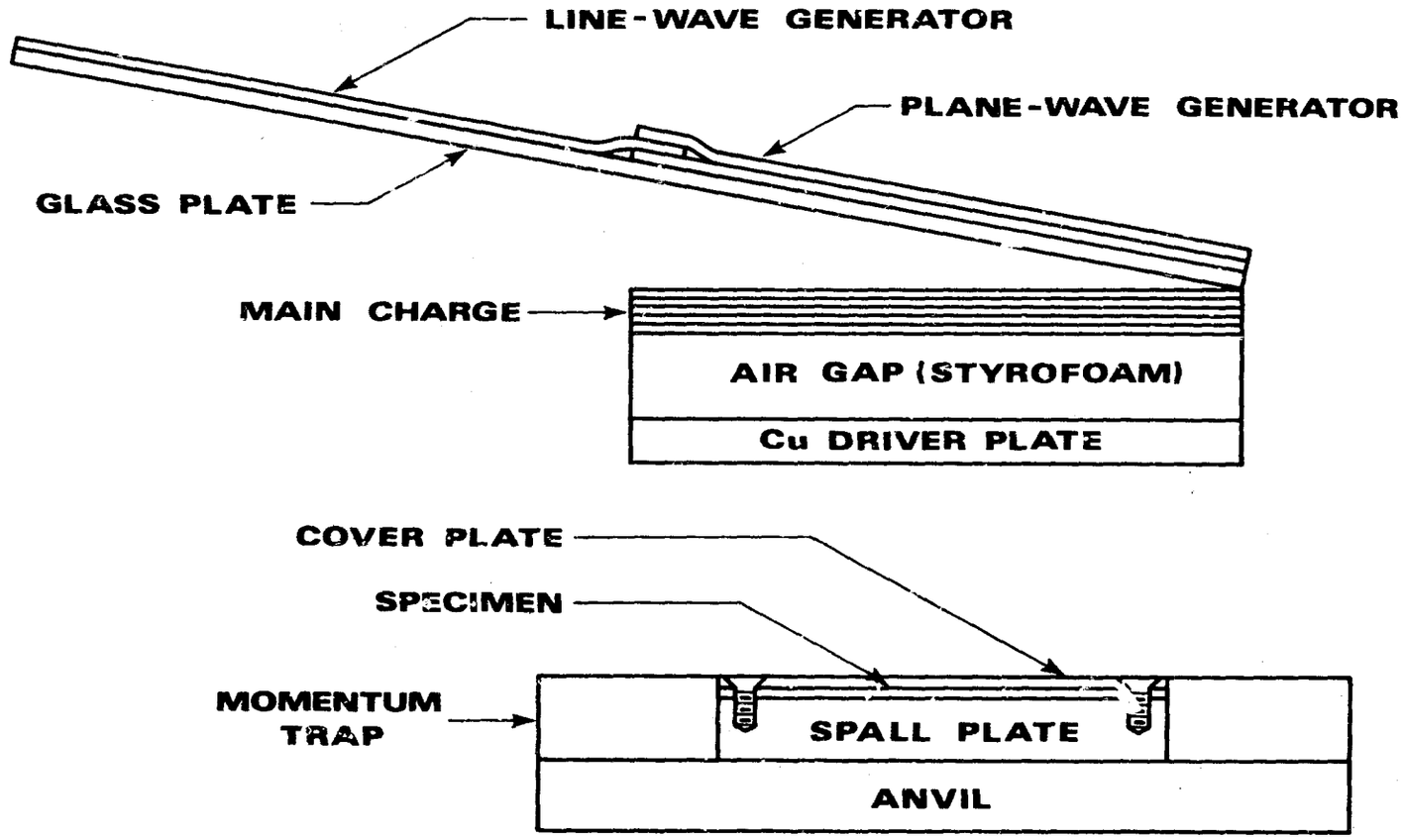

Figure 2. Shock-Loading Assembly

high-velocity impact with the specimen assembly shown at the bottom of Figure 2, and also in Figure 3. This system is designed to prevent spalling and to minimize internal wave reflections and their concomitant effects. It consists of a 1/8-in. thick steel cover plate to protect the specimen surface and a 3/4-in. thick spall plate. In between, a 4 in. by 5 in. specimen is secured by screws at the periphery. This composite, surrounded by four 1-in. thick momentum traps, rests on a 3/4-in. thick steel anvil plate. The various components are adhered together tightly by means of an epoxy resin to ensure transmittal of the shock wave across metal/metal interfaces. All of the steel is hot-rolled AISI 1014, the acoustic impedance of which closely matches that of Udimet 700. Consequently, the amplitude of rarefaction waves at the specimen surfaces is negligible.

The driver is a 6 in. by 7 in. plate of copper which is accelerated to a constant velocity through a 0.5-in. air gap (standoff distance) by the main explosive charge. The plane-wave system, used to detonate this explosive uniformly, is comprised of Plexiglas wedges supporting a glass plate at an angle of 11°15'. Onto this is glued a line wave charge diverging to two sheets of explosive. Point detonation of the former results in the line detonation of the latter. In turn, as the two sheets burn, they fracture the glass. The set angle provides a planar shower of glass fragments onto the main charge. This results in simultaneous detonation over its whole surface.

The explosive, a DuPont PETN-base plastic variety with a density of 2 g/in^2, is known commonly as "Detasheet C-2." The detonation velocity is given by the manufacturer as 7000 msec. (Very recent measurements here[38] have yielded an average value of 7380 msec, about 5% higher.) Of the 2 g/in^2, only 63% is PETN while 8% is nitrocellulose. Thus, 71% of C-2 can be considered to be active explosive with the rest being binder.

One can determine the explosive charge necessary for a prescribed shock pressure in one of three ways: (1) by calculation, knowing the Hugoniot relations for the specimen and driver, and the velocity of the driver as derived from the mechanics of plate acceleration; (2) by direct measurement; (3) by comparison with previously measured shock-loading parameters. The Hugoniot relation for Udimet 700 has not been determined. Although a composite curve has been constructed (Section 4.4) from those for the individual elements, the complexity of the microstructure precludes confidence in its accuracy without

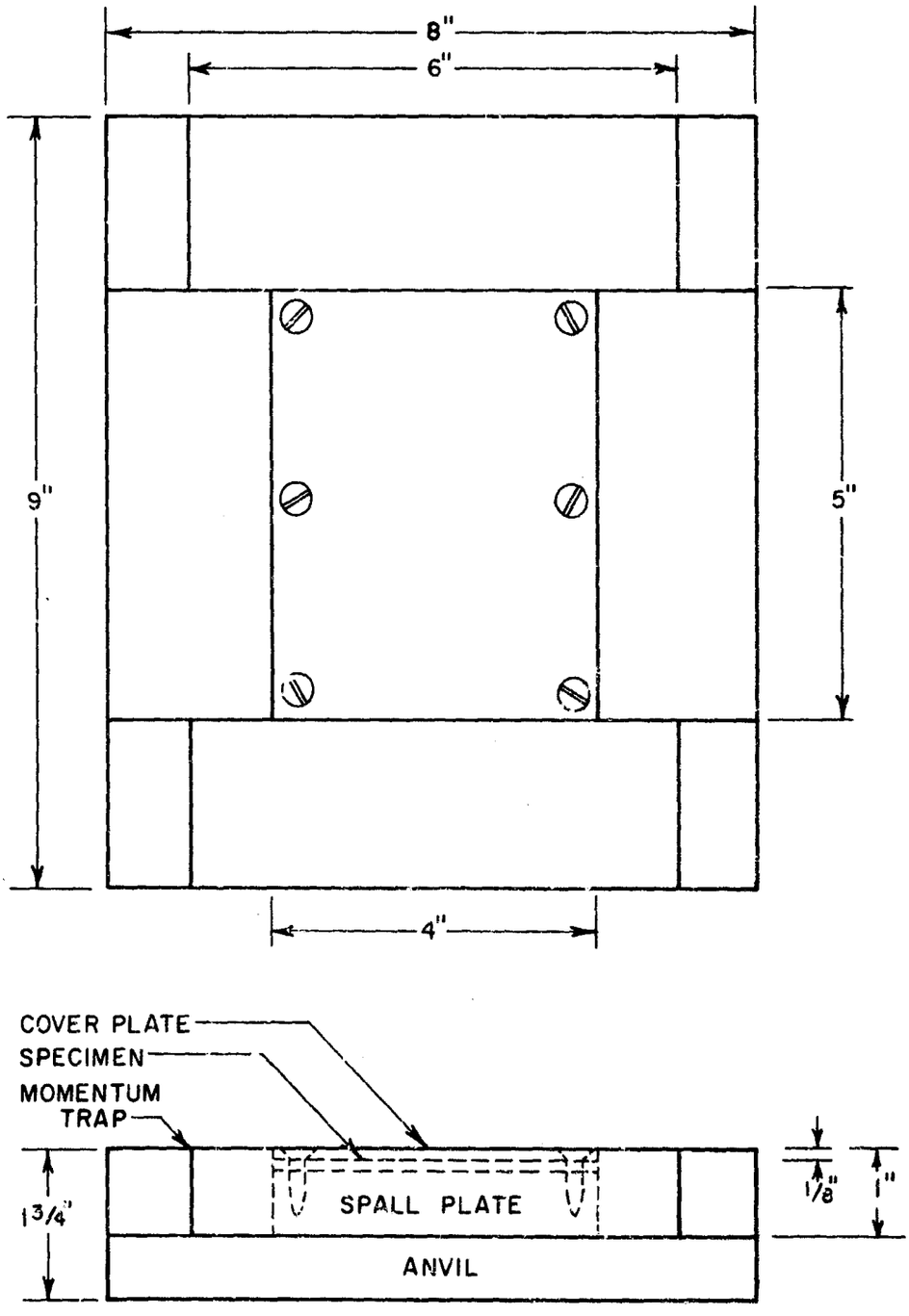

Figure 3. Specimen Assembly: Rectangular Plate Geometry

experimental confirmation. Direct measurement has been time-consuming and costly. However, advanced probe techniques presently being established at this laboratory will permit the less expensive measurement of driver plate velocity, and shock velocity at top and bottom surfaces of a specimen[38]. Nevertheless, the charge requirements were calculated by using the data generated by Holtzman and Cowan[26] for austenitic manganese steel. This has a density of 0.236 lb/in^3, identical to that for Udimet 700. With the same driver plate thicknesses, one need compare only detonation velocities and the weight of explosive.

The shock pressure is determined then by utilizing the data in Table 1 of Reference 26. The correct comparison for the weight of explosive is between the PETN weight given in the above table divided by the area of the explosive sheet (25 in^2), and 71% of the density of C-2 "Detasheet" used in this investigation. A sample calculation, then, provides a shock pressure, in kbar, of

$$P = \frac{2(0.71)N}{153/25} \times \frac{7000}{7300} \times 70 = 15.57N$$

where N = number of sheets of C-2. Thus 5 sheets of C-2 gives a shock pressure of 78 kbar. The shock conditions for this study are summarized in Table 2. The pressures can be considered to be accurate to about 5%[26].

Table 2. Shock-Loading Parameters

Weight of Explosive (g)	No. of Layers of C-2	Thickness of Cu Driver (in.)	Velocity of Driver (m/sec)	Shock Pressure (kbar)
294	5*	0.485	412	78
118	2	0.120	1310	287
732	14	0.120	2140	527

* 1-in. air gap (styrofoam) between explosive and driver

A view of the whole shock-loading system is shown in Figure 4. As indicated in the figure, the assembly is placed on a piece of insulation board set on a cardboard barrel filled with water. The water

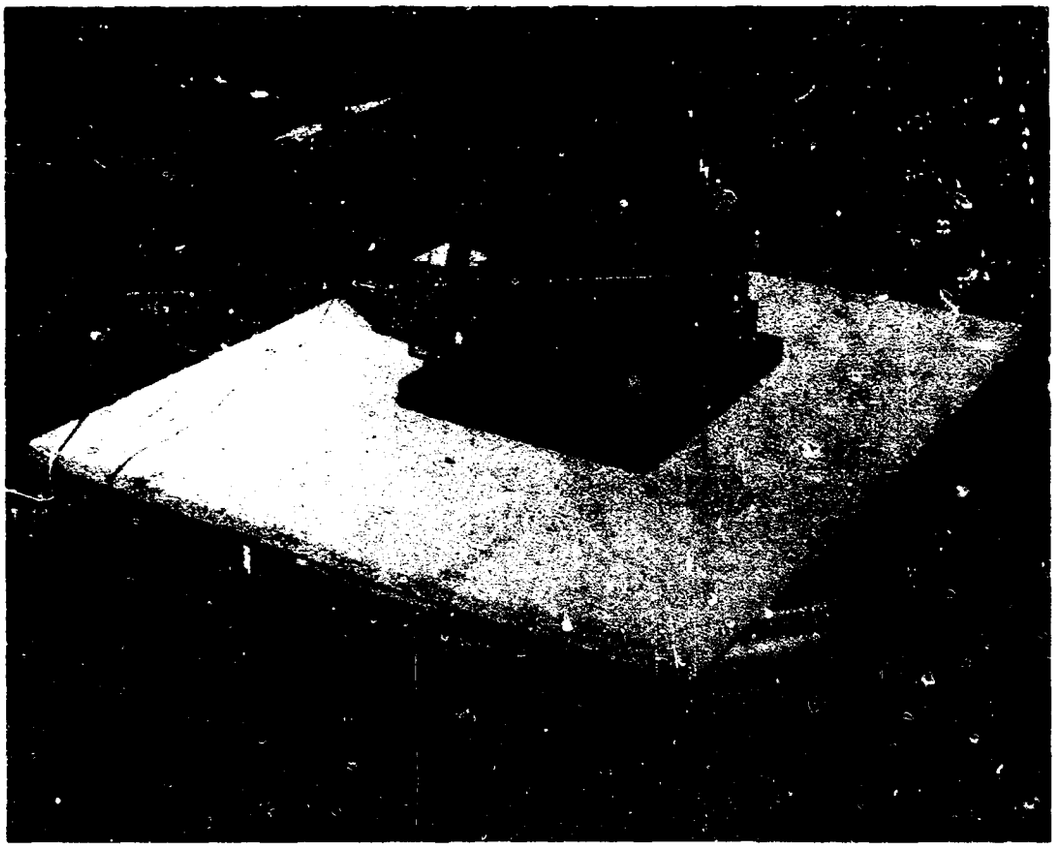

Figure 4. Shock Assembly in Position for Detonation

serves both as a deceleration and quenching medium. At high shock pressures, the steel anvil experiences severe spallation, but in all cases the spall plate/specimen/cover plate composite is recovered intact from a pool formed by some of the water originally in the barrel.

Three disc specimens, 0.150 in. thick and 4.75 in. diameter, of an experimental proprietary nickel-base alloy, PM-101, were shocked for AVCO, Lycoming Division -- one at 527 kbar and two at 413 kbar. The specimen arrangement used for shock loading, with plane-wave generation, is shown in Figure 5. It should be pointed out that this "bathtub" system is not quite as suitable as one which would permit free lateral motion of the surrounding steel momentum cylinder; high residual strains result from impact. That is, the disc specimen should be placed upon a spall plate of the same diameter, and in turn, surrounded by a split momentum cylinder to absorb the lateral energy and inhibit wave reflections at the specimen edges. However, this arrangement is more expensive to fabricate than the one illustrated in Figure 5. The Rockwell C hardness data in Table 3 demonstrate the average shock hardening achieved. Further information on the result of subsequent aging treatments on terminal properties of this alloy may be obtained directly from AVCO.

Table 3. Effect of Shock Loading on Hardness of AVCO PM-101 Nickel-Base Alloy

History	Initial Hardness (Rc)	Shock Pressure (kbar)	Shocked Hardness (Rc)
As-Forged	49.6	527	57.7
Solution Treated	48.3	413	54.2
Solution Treated	46.9	413	53.1

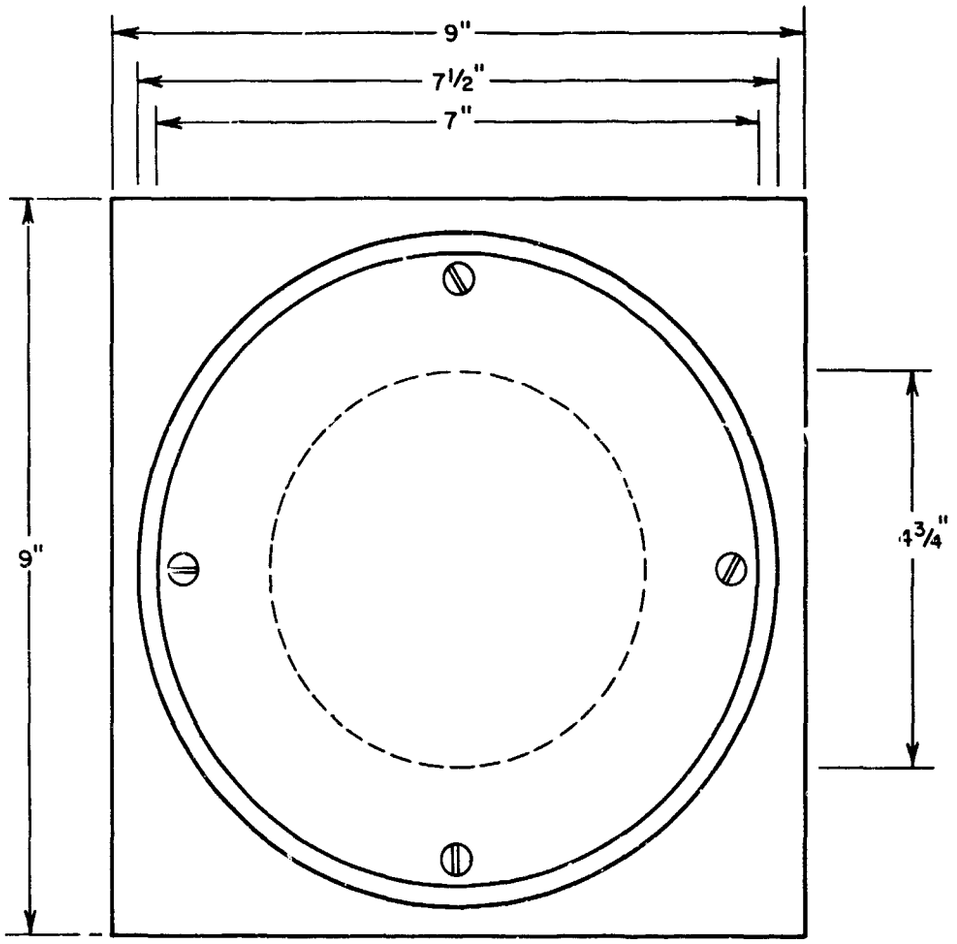

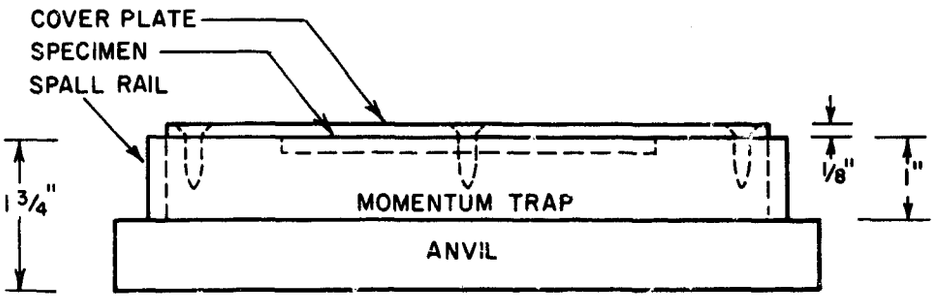

Figure 5. Specimen Assembly: Pancake Geometry

4.4 Shock Wave Relations for Udimet 700

Composite parametric equations describing the shocked state of Udimet 700 were calculated from the known characteristics of its alloying constituents. Starting with the empirical relation[27,39,40] between particle velocity, u, and shock velocity, U, for each element, i.e.,

$$U = C_i + S_i u, \tag{2}$$

with partitioning based on the atomic fraction, a, the elemental contributions, designated C_i' and S_i', were determined simply from

$$C_i' = a_i C_i \text{ and } S_i' = a_i S_i . \tag{3}$$

The final equation is

$$U = C + Su \tag{4}$$

where

$$C = \Sigma C_i' \text{ and } S = \Sigma S_i' . \tag{5}$$

Values of C_i and S_i for the alloying elements in Udimet 700 are listed in Table 4. Data for boron were not found, but its low concentration permits its exclusion with little error. The nickel content was corrected for this omission.

Table 4. Determination of Constants C and S in the Relation Between Shock Velocity and Particle Velocity for Stellite Udimet 700 Sheet

Element	C_i	S_i	Atomic Fraction	C_i'	S_i'	Ref.
Al	5.38	1.337	0.0908	0.488	0.121	41
C	3.86	1.98	0.0046	0.017	0.009	42
Co	4.740	1.392	0.1345	0.637	0.187	43
Cr	5.249	1.445	0.1672	0.878	0.241	43
Mo	5.120	1.285	0.0270	0.138	0.035	43
Ni	4.796	1.254	0.5358	2.570	0.672	43
Ti	4.590	1.259	0.0402	0.185	0.051	43

$C = \Sigma C_i' = 4.913$ $\quad S = \Sigma S_i' = 1.316$

The partitioning of elements to γ and γ' was determined by Kriege and Baris[44] for material which was not fully heat treated (136 hrs at 1800°F). The coefficients in Eq. 4 were evaluated for γ and γ' phases, and for Stellite sheet and commercial material assuming all alloying constituents were in solution. These are listed in Table 5. The values of C and S for γ and γ' differ by less than 3% from those for the solid solution. Thus, although shock-wave propagation in Udimet 700 could be expected to be influenced by the presence of γ', the solid solution case should provide a reasonable estimate of the shock-wave relations. For Udimet 700 then,

$$U = 4.913 + 1.316u \text{ mm}/\mu\text{sec} . \tag{6}$$

Table 5. Values of C and S for Udimet 700

Phase	Material	Investigation	C	S
Solid Solution	Stellite Sheet	Present	4.913	1.316
Solid Solution	Commercial	Kriege and Baris (44)	4.912	1.320
Gamma	Commercial	Kriege and Baris (44)	4.933	1.338
Gamma Prime	Commercial	Kriege and Baris (44)	4.871	1.282

The relationship between the shock pressure P and u, or P and U, can be obtained from the equation for conservation of momentum:

$$P = \rho_0 U u \tag{7}$$

where ρ_0 is the density in the unshocked state. Combining Eqs. 4 and 7 with

$$\rho_0 U = \rho (U - u), \tag{8}$$

the requirement that mass be conserved, yields an expression which permits the construction of a Hugoniot curve (P vs. V/V_0). That is,

$$P = \frac{C^2 (V_0 - V)}{[V_0 - S(V_0 - V)]^2} . \tag{9}$$

Substitution of appropriate values of C and S from Eq. 6, and the initial density of 7.91 g/cm ($= 1/V_0$), results in the curve for Udimet 700 shown in Figure 6.

The U vs. u relation for Udimet 700, Eq. 6, can be compared with

$$U = 4.796 + 1.254u \tag{10}$$

for nickel[43], the base element. This, in turn, yields the Hugoniot curve for nickel in Figure 6.

4.5 Determination of Strains

The Hugoniot curve in Figure 6 permits a calculation of the transient shock strain, using Eq. 1 for natural strain, $\bar{\epsilon}_s$, or

$$\epsilon_s^* = \frac{4}{3}\left(\frac{V_0 - V}{V_0}\right) \tag{11}$$

for engineering strain. This derives from the following relation for effective or generalized strain[45],

$$\epsilon^* = \frac{\sqrt{2}}{3}\left[(\epsilon_1 - \epsilon_2)^2 + (\epsilon_2 - \epsilon_3)^2 + (\epsilon_3 - \epsilon_1)^2\right]^{\frac{1}{2}} \tag{12}$$

substituting $\epsilon_1 = -\epsilon_{ts}$, the thickness strain, and $\epsilon_2 = \epsilon_3 = 0$ for zero lateral displacement; the rarefaction component doubles the value. The magnitudes of transient strain corresponding to the applied shock pressures, and the measured average residual strains, are listed in Table 6. The equivalent percent reductions in thickness by cold rolling are included. These were calculated by requiring the effective rolling strain to be equal to ϵ_s^*, the transient shock strain, and solving Eq. 11 for ϵ_{tr} where $\epsilon_1 = -\epsilon_{tr}$, $\epsilon_2 = \epsilon_{tr}$, and $\epsilon_3 = 0$.

Thus,

$$\epsilon_{tr} = \frac{\sqrt{3}}{2}\epsilon_s^* . \tag{13}$$

The value of V/V_0 for the lowest shock pressure was originally read incorrectly from the Hugoniot curve at 39 kbar instead of at 78 kbar.

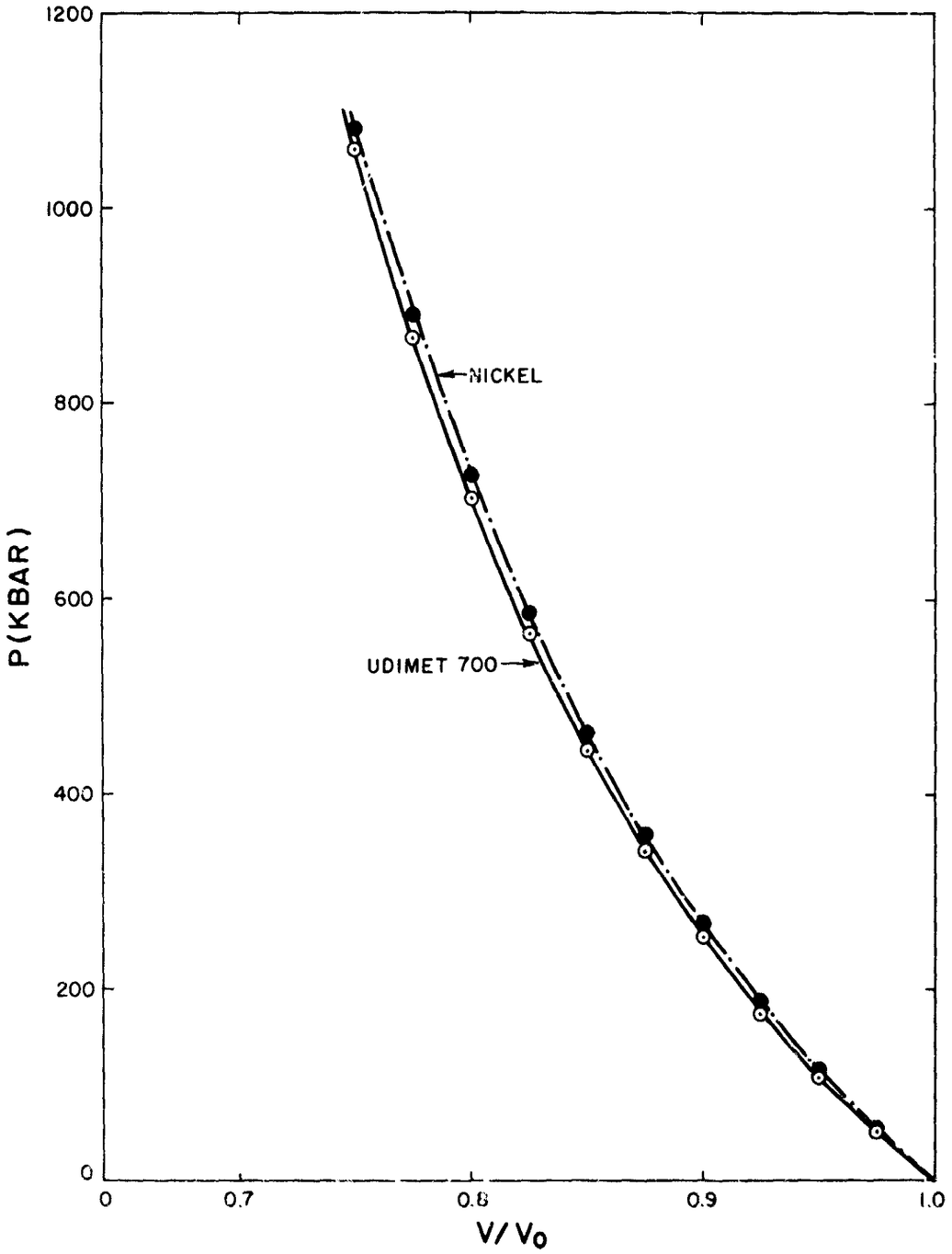

Figure 6. Hugoniot Curves for Nickel and Udimet 700

Consequently, the comparison with rolled material was made at 1.4% thickness reduction instead of 4.2%, the value in Table 6. This affects only the hardness comparisons at the lowest shock pressure. It was felt that since the shock-aging process was the more important, a repetition of this set of heat treatments was not justified.

Table 6. Transient and Residual Shock Strains and Equivalent Rolling Reductions

Shock Pressure (kbar)	Transient Strain (Percent)	Equivalent Thickness Reduction by Rolling (Percent)	Measured Residual Strain (Percent)
78	4.8	4.2	0.6
287	14.4	12.5	0.7
527	22.1	19.1	2.0

On the other hand, this lower strain permits an assessment of the relative effect of a rolling strain equivalent to the residual shock strain. Due to the lateral expansion components of the residual strain, the effective residual strain, from Eq. 11, is equal simply to the thickness reduction, e.g., 2.0% for 527 kbar. The effective rolling strain corresponding to 1.4% thickness reduction is 1.7%, a value close to the residual strain at 527 kbar.

4.6 Testing Procedures

Relative strength levels at room temperature were monitored by means of macrohardness (Rockwell C, 150 kg. load) and microhardness (diamond pyramid, DPH, 10 kg. load) measurements. The latter were obtained by means of a Tukon hardness tester. The Rockwell tests permitted the collection of hardness data at all stages of deformation and heat treatment without the more extensive surface preparation necessary for microhardness tests.

Elevated-temperature tensile tests in air were conducted with a floor-model 10,000-lb capacity Instron universal testing machine at a strain rate of 3×10^{-4} sec^{-1} (cross-head speed = 0.02 in./min.).

Temperature was controlled by means of a chromel-alumel thermocouple in close proximity to the specimen at the gage section. Stress-rupture life and ductility were evaluated at constant load by means of a Satec creep machine. Temperature was again monitored by means of a thermocouple near the specimen surface.

Identical specimen geometry was used for both tensile and rupture tests. These specimens had a gage length of one inch, gage width of 0.150 in., and were cut with their axis parallel to the original and TMP sheet rolling direction.

5. RESULTS AND DISCUSSION

5.1 Hardness

The room temperature hardness of stellite Udimet 700 sheet which had undergone shock deformation and subsequent aging was compared with that of material which was cold-rolled and aged, and which was thermally processed without mechanical working. Rockwell "C" hardnesses are recorded in Tables 7 thru 9 for as-deformed and aged Udimet 700 with predeformation histories A (ST), B (ST + γ'), and C (ST + γ' + C), respectively. The effect of shock TMP and conventional TMP on hardness is illustrated in Table 10 by the percentage differences from normally heat treated controls. This table includes the percentage differences in hardness between shock-processed and conventionally-processed Udimet 700. The last column provides a comparison between the average residual shock strain of 2.0% corresponding to a pressure of 527 kbar (Table 6), and an effective rolling strain of 1.7% From a more practical standpoint, the departures in hardness from the fully heat treated condition (STA) introduced by TMP are shown in Table 11.

Certain consistent trends are evident from the data. Firstly, cold work, whether applied quasi-statically by rolling, or at an ultra-high rate by shocking, results in a room temperature strengthening effect in Udimet 700, irrespective of the initial history. Moreover, as would be expected, this work hardening increases with increasing rolling strain, transient shock strain, or shock pressure. This point is further demonstrated for the shock case by the curves in Figure 7 where the percentage increase in hardness is plotted against shock pressure. The shock-hardening behavior is consistent with that found previously for unalloyed nickel, Inconel 600, Chromel-A, TD-Ni, and TD-NiCr[46]. The increase in microhardness (DPH) from the unshocked state (~360) to the shocked condition (~470) after the application of a pressure pulse of 527 kbar is slightly over 100 DPH. This is approximately the same as the increase experienced by TD-Ni and TD-NiCr shocked to 460 kbar. The rise in hardness is roughly doubled (~200 DPH) for Inconel 600 and Chromel A. Whether nickel falls in the former[47] or latter[46] category depends on which of two papers by Murr and his coworkers[46, 47] one favors. Since the initial hardness of Udimet 700 appreciably exceeds that of the aforementioned alloys, the, fractional strengthening displayed by shock-loaded Udimet 700 will be less than that exhibited by the other materials, as shown by their

Table 7. Hardness Data (Rc) for Udimet 700 Deformed in Solution-Treated Condition (History A)

Deformation History	Shock Pressure (kbar)	Effective Strain (Percent)	As-Deformed	Aging Treatments						
				γ'	γ'+C	γ'+F	γ'+C+F	C	C+F	F
U		0	38.3*	36.4	35.9	36.2	36.6	38.7	39.7	40.0
R		1.7	40.1	38.3	37.3	40.8	40.2	41.2	40.9	45.3
S	78	4.8	39.4	38.6	38.7	41.5	40.5	40.1	41.3	42.8
R		14.4	46.3	39.4	40.4	44.0	41.9	45.2	43.0	47.1
S	287	14.4	40.9	39.3	39.7	42.8	41.4	41.3	42.5	43.9
R		22.1	48.7	41.7	41.4	44.9	44.1	45.9	46.9	49.2
S	527	22.1	47.3	40.3	42.0	44.8	44.0	42.8	44.1	47.5

* solution treated

Table 8. Hardness Data (Rc) for Udimet 700 Deformed in ST + γ' Condition (History B)

Deformation History	Shock Pressure (kbar)	Effective Strain (Percent)	As-Deformed	Aging Treatments C	C+F	F
U		0	37.2*	40.3	41.3	41.0
R		1.7	40.3	40.2	43.5	43.6
S	78	4.8	39.5	41.6	42.2	42.6
R		14.4	46.9	42.9	45.2	47.7
S	287	14.4	40.8	42.4	43.5	45.0
R		22.1	48.8	45.5	45.7	48.0
S	527	22.1	47.0	43.6	44.6	45.8

* solution treated and γ' aged

Table 9. Hardness Data (Rc) for Udimet 700 Deformed in ST + γ' + C Condition (History C)

Deformation History	Shock Pressure (kbar)	Effective Strain (Percent)	As-Deformed	Aging Treatment F'
U		0	38.4*	41.3
R		1.7	42.5	42.7
S	78	4.8	42.0	43.3
R		14.4	48.2	45.7
S	287	14.4	42.7	44.9
R		22.1	49.3	48.3
S	527	22.1	49.4	47.0

* solution treated, γ' and carbide aged.

Table 10. Percentage Change in Hardness (Rc) of Udimet 700 Due to Shock or Conventional TMP

Schedule	Shocked-Undef. / Undef (Percent)			Rolled-Undef. / Undef. (Percent)			Shocked-Rolled / Rolled (Percent)		
	78	287	527	1.7	14.4	22.1	287 (14.4)	527 (22.1)	527 (1.7)
A (As-Def.)	2.9	6.8	23.5	4.7	20.9	27.2	-12.1	-2.9	17.9
A1	6.0	8.0	10.7	5.2	8.2	14.5	- 0.3	-3.4	5.2
A2	7.8	10.6	17.0	3.9	12.5	15.3	- 1.7	1.4	12.6
A3	14.6	18.2	23.7	12.7	21.5	23.8	- 2.7	-0.2	9.8
A4	10.7	13.1	20.2	9.8	14.5	20.5	- 1.2	-0.2	9.5
A5	3.6	6.7	10.6	6.5	16.8	18.6	- 8.6	-6.7	3.9
A6	4.0	7.1	11.1	3.0	8.3	18.1	- 1.6	-6.0	7.8
A7	7.0	9.7	18.7	13.2	17.8	23.0	- 6.8	-3.5	4.9
B (As-Def.)	6.2	9.7	26.3	8.3	26.1	31.2	-13.0	-3.7	16.6
B5	3.2	5.2	8.2	- 0.2	6.5	12.9	- 1.2	-4.2	8.5
B6	2.2	5.3	8.0	5.3	9.5	10.7	- 3.8	-2.4	2.5
B7	3.9	9.8	11.7	6.3	16.3	17.1	- 2.7	-4.5	5.0
C (As-Def.)	9.4	11.2	28.7	10.7	25.5	28.4	-11.4	0.2	16.2
C7	4.8	8.7	13.8	3.4	10.6	16.9	- 1.8	-2.7	10.1

Table 11. Percentage Change in Hardness (Rc) of Udimet 700 Due to Shock or Conventional TMP Relative to Full Heat Treatment (STA)

Schedule	Shocked - STA / STA (Percent)			Rolled - STA / STA (Percent)		
	78	287	527	1.7	14.4	22.1
A (As-Def.)	7.7	11.8	29.3	9.6	26.5	33.1
A1	5.5	7.4	10.1	4.6	7.7	13.9
A2	5.7	8.5	14.8	1.9	10.4	13.1
A3	13.4	16.9	22.4	11.5	20.2	22.7
A4	10.7	13.1	20.2	9.8	14.5	20.5
A5	9.6	12.8	16.9	12.6	23.5	25.4
A6	12.8	16.1	20.5	11.7	17.5	28.2
A7	16.9	20.0	29.8	23.8	28.7	34.5
B (As-Def.)	- 4.4	2.7	13.8	- 2.4	13.6	18.2
B5	0.7	2.7	5.6	- 2.7	3.9	10.2
B6	2.2	5.3	8.0	5.3	9.4	10.7
B7	3.1	9.0	10.9	5.6	15.5	16.2
C (As-Def.)	1.7	3.4	19.6	2.9	16.7	19.4
C7	4.8	8.7	13.8	3.4	10.7	17.0

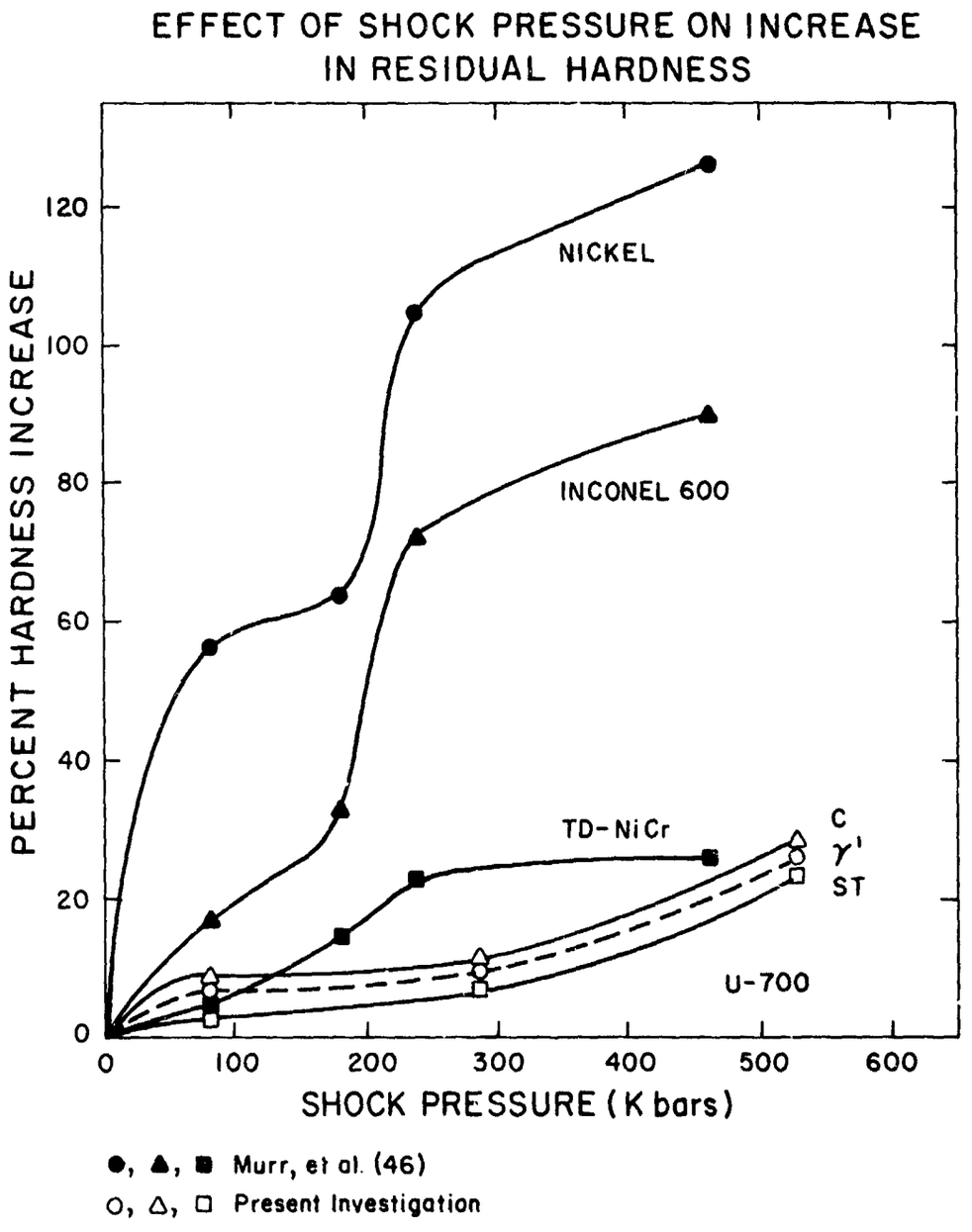

Figure 7. Shock-Hardening Curves for Several Nickel-Base Alloys

hardening curves in Figure 7. One can see from the figure that the three different histories yield almost parallel shock-hardening curves. Even on an absolute scale, the substructure strengthening can be considered to be independent of the degree of aging.

A second noteworthy feature of the observations is evident from Table 10 where the comparison of hardness after TMP is made with material which has not been strained but has otherwise undergone exactly the same thermal treatment; thus the normal response to aging is factored out. The results show that the strengthening effect is maintained to various degrees, by aging subsequent to deformation. Also, the strain sensitivity of the strengthening remains positive throughout. The single exception is the value for schedule B5 after 1.7% effective rolling strain. Essentially no change (-0.2%) from undeformed material was detected by macrohardness measurements; the DPH value increased 12 points or nearly 4%. The bar graphs in Figure 8 demonstrate the improvements in room-temperature strength that can be introduced by shock (527 kbar) and conventional TMP (19.1% rolling reduction) as reflected by hardness data.

A third point which warrants discussion is the fact that the ambient temperature strengthening brought about by shock loading to a pressure of 287 or 527 kbar is almost invariably less than that achievable by rolling an amount equivalent to the corresponding transient shock strain. This is shown by columns 7 and 8 in Table 10, and for the highest strain, by the bar graphs in Figure 8. The two exceptions are schedules A2 and C, where the hardness of shock-processed Udimet 700 is slightly greater than after conventional TMP. When shocked and rolled hardnesses, on the other hand, are compared on the basis of residual strain, then it is evident from the last column of Table 10 that the strength improvements which can be obtained by shock-aging cannot be matched by conventional means when the dimensional changes which can be tolerated are very small.

The hardness data do not permit any decision concerning the mechanisms responsible for the observed TMP strengthening effects. Nevertheless, a further analysis of the data led to the tentative conclusion that a dislocation substructure alone cannot account directly for all of the hardening. For example, shock hardening at 527 kbar raised the hardness in the solution-treated condition by Rc 9.0. Thermal recovery during subsequent γ' aging reduced this by 5.1,

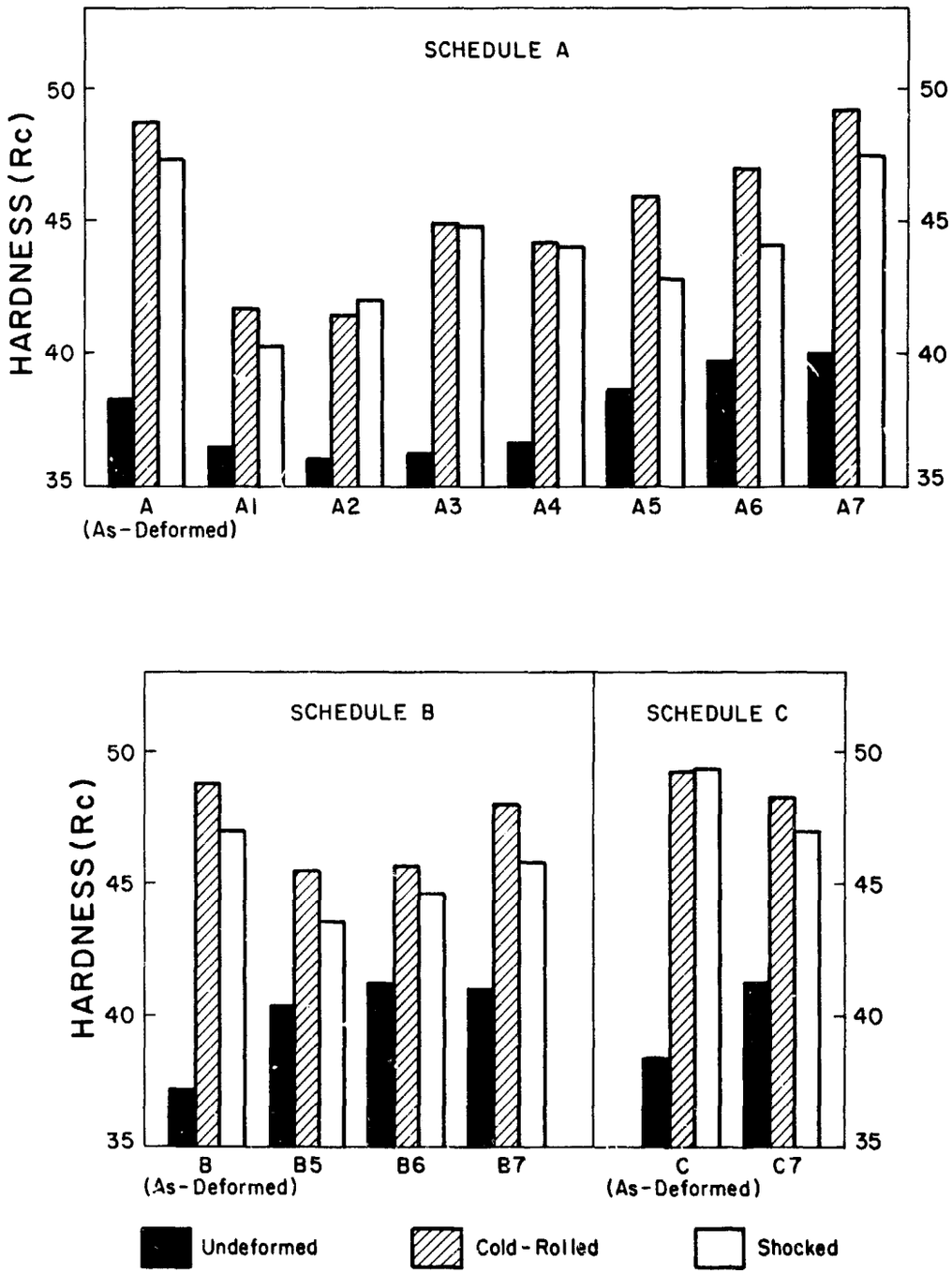

Figure 8. Comparison of Hardness (Rc) of Udimet 700 Following Thermal Processing, Conventional TMP by Rolling (19.1% Reduction), and Shock TMP (527 kbar)

or 57%. However, an additional carbide plus a final age (A4) restored Rc 3.5 of this loss, to 82% of the original hardness difference. Moreover, a final age without an intervening carbide age (A3) brought this up even higher to Rc 8.6, or 96% of the original. Thus, the interaction of dislocations with the prestrain-induced dislocation substructure probably accounts for about one-half of the hardness increase for schedule A4. The remainder is necessarily a result of the terminal defect structure, but a more indirect one associated with the role that it plays in the modification of other aspects of the overall microstructure.

When the final aging treatment at 1400°F is the only one which is applied to the AS and AR schedules, about 85% remains of the strengthening introduced originally by working. Since thermal recovery effects are not as extensive as those during a 1975°F age, one could reasonably expect nearly all of the 85% to be a substructure contribution. However, in the B and C schedules, the 527 kbar shock hardening left after converting to B7 and C7 by final aging was lower than for A7, at 49% and 52%, respectively. This suggests again that substructure strengthening per se probably constitutes only about half of the 85% figure. It seems that the final aging treatment leads to certain microstructural changes which are beneficial to room temperature strength when deformation is imparted in the solution treated condition and moreover, when the intermediate γ' and carbide aging steps are omitted from the postdeformation heat treatment schedule.

From the preceding discussion and results, the final aging process stands out as the one which may be the most important to shock-age or strain-age strengthening. Conversely, the hardness data also demonstrate that the carbide age at 1550°F is the one which could be considered the most detrimental -- in the sense that its effect on reducing the strength due to work hardening cannot be overcome by subsequent aging, i.e., by the final aging treatment.

Confirmation of these views and the determination of the operative TMP strengthening mechanisms will require high-resolution structure characterization by surface replication and thin foil techniques. These studies are presently underway.

The hardness measurements served another purpose. The large number of TMP schedules precluded the evaluation of the effect of each on elevated temperature short-term tensile and stress-rupture properties. Hardness was used as one method of screening,

supplemented by optical metallography. The percentage differences in Table 11 furnish a more realistic view of the influence of TMP since they were all calculated relative to fully heat treated (STA) material, i.e., what would normally be the standard service condition. Ultimately, three TMP schedules were selected, one for each predeformation history A, B, and C. The choice of A6 over A7, despite its less favorable strength characteristics at room temperature, was dictated largely by logic. It was reasoned that a final age by itself would not be sufficient to produce the grain-boundary carbides ($M_{23}C_6$) necessary for the high creep resistance of Udimet 700. The choice of A6 over A3, again despite less hardening, was made because of the occurrence, during the 4 hour γ' age at 1975°F, of a cellular reaction as discussed in the next section (Section 5.2). A third consideration was the fact that A6 corresponded to one of the two schedules investigated by Blankenship[19, 20]. Although he claimed that his choice was arbitrary, one suspects that it was governed, to some degree at least, by similar reasoning.

The decision to use schedule B7 instead of B5 or B6 was due to two factors. It exhibited the highest hardness, and it counteracted the selection of A6 over A7. The contention was that a comparison of A6 and B7 could provide some information about the significance of eliminating the carbide aging step.

5.2 Microstructure

The influence of conventional and shock TMP on the microstructure of Udimet 700 was examined by optical metallography and by the electron microscopy of surface replicas. The results of transmission studies currently in progress will be reported in the near future.

One of the most striking effects of shock loading relative to rolling in the stability that is apparently imparted to the microstructure by the former operation. Figure 9(a) shows evidence of the occurrence of recrystallization. This is manifested by the formation of a cellular precipitate during aging at 1975°F for 4 hours. Such a cellular reaction was observed whenever the γ' aging step followed cold rolling in the solution treated condition to reductions of 12.5 or 19.1%. Thus, this holds for schedules AR1 to AR4 inclusive. Cellular recrystallization has been observed previously[48] in cold-reduced Udimet 700 annealed thereafter at 1800°F for 16 hours. In that investigation, as in the present one, the average particle size of the cuboidal γ' was about the same, namely, 1600 and 1650Å, respectively, prior to deformation.

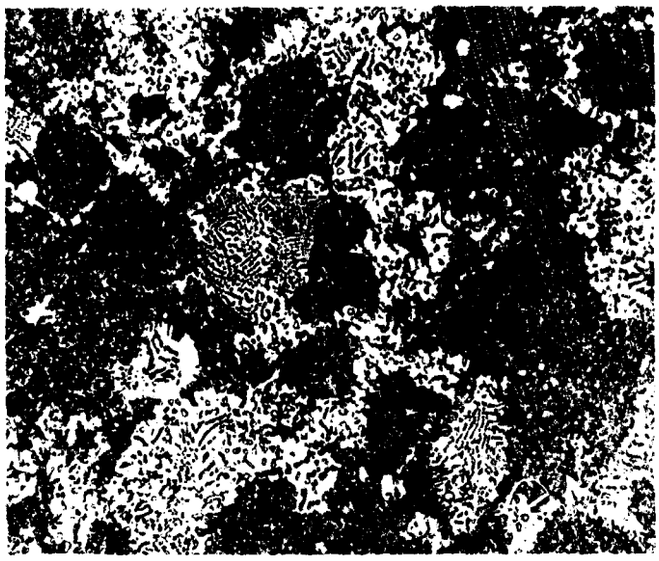

a. Cold Rolled to 12.5% Reduction in Thickness; 500X

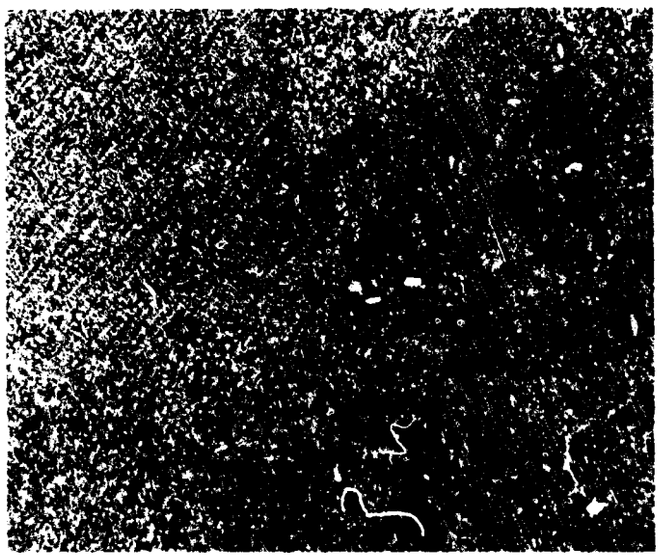

b. Shock Loaded to 287 kbar; 500X

Figure 9. Cellular Precipitate in Udimet 700 Aged at 1975°F for Four Hours Following Cold Work in the Solution Treated Condition.

As a point of interest, the γ' matrix within the recrystallization cells contained a fine dispersion of secondary γ' with an average size of about 1000Å. The primary γ' had coarsened to about 3000Å.

In direct contrast to the above findings, cellular recrystallization was not detected in any of the shock-loaded material. The photomicrograph in Figure 9(b) typifies microstructures resulting from the γ' aging of shock-hardened Udimet 700.

A number of questions remain unanswered at this stage of the investigation. One is led to inquire whether the preceding shock-induced stabilization would be transferred to shock TMP schedules wherein the heat treatment is more complete, say AS4 or AS6, and which schedules would exhibit the most benefit. Concurrently, it would be of interest whether elevated temperature mechanical properties are favorably affected. Certainly, one would like to know why shock deformation impedes the cellular reaction.

One factor which could play a substantial role in governing the propensity for cellular recrystallization is the homogeneity of the defect structure introduced by prior cold work. Figure 10 suggests that the dislocation substructure is far more uniformly distributed in shocked than in rolled Udimet 700. Slip bands are revealed dramatically in Figure 10(a) by the appropriate etching of a solution treated and rolled sample. Slip bands have been reported[20,48] before in Udimet 700 with a γ' particle size similar to that measured in the Stellite sheet on air cooling from the solution treatment temperature of 2150°F. Conversely, identical metallographic preparation failed to disclose deformation markings in material which was solution treated and shocked at 527 kbar, as in Figure 10(b), or at the two lower pressures. The slip bands in rolled material can still be delineated by etching after carbide or final aging treatments or both. Moreover, some fine, closely-spaced slip striations were detectable in shock specimens after a final age at 1400°F. Although confirmation is necessary, it is conceivable that in this case $M_{23}C_6$ carbides have nucleated on dislocations rendering the slip structure visible. However, no deformation markings could be discerned when γ' aging or carbide aging preceded rolling or shock loading, i.e., for predeformation histories B and C. This agrees with previous findings for Schedule CR[20].

a. Cold Rolled to 19.1% Reduction in Thickness; 250X

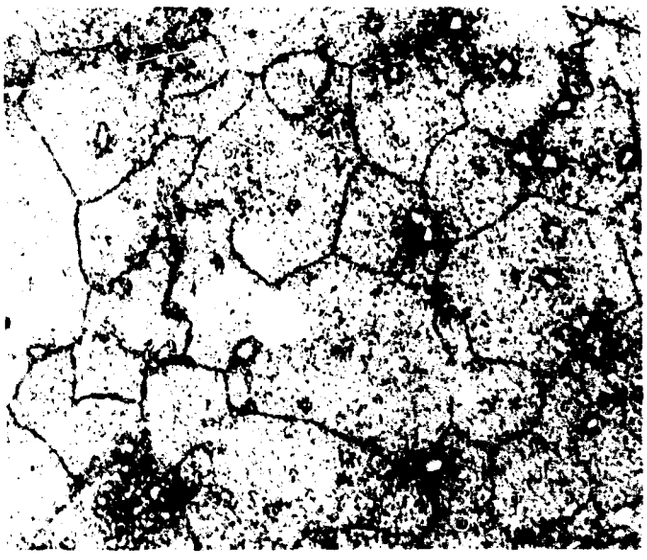

b. Shock Loaded to 527 kbar; 250X

Figure 10. Macroscopic Character of Slip in Solution Treated and Deformed Udimet 700.

The result of prior cold work, at conventional or shock rates, on γ' morphology and distribution is typified by the microstructures in Figure 11 which provides a comparison between thermally processed and shock processed Udimet 700. Instead of the common well-defined cuboidal form, the morphology is distorted during coarsening at 1975°F to a more spheroidal geometry. In addition, the normal alignment along <100> appears to be obscured. Lastly, the particle size is about 30% smaller and the spacing reduced when deformation precedes γ' aging.

Other microstructural changes will be discussed in subsequent sections insofar as they relate to elevated temperature mechanical properties.

5.3 Elevated Temperature Tensile Properties

The tensile properties of Stellite Udimet 700 sheet were evaluated at 1200°F for schedules A6, B7, and C7. The examination of C7 simply satisfies the expressed desire to have all three predeformation histories represented. This schedule coincides with the second (B) of two investigated by Blankenship and Gyorgak[19, 20]. The influence of shock TMP utilizing a 527 kbar pressure pulse was compared with the properties of fully heat treated control material, designated STA in the tables, and with the effects of conventional TMP achieved by cold rolling to a 19.1% thickness reduction. These values of pressure and rolling strain were used because they were found to yield the greatest room temperature residual hardening.

The tensile data are listed in Table 12. The underlined values are the means for two tests at a given condition. These results are displayed in the form of bar graphs in Figure 12 and 13. The advantage of the insertion of a cold working step, irrespective of the deformation rate, on the strength at 1200°F is clearly indicated. This is further emphasized quantitatively by the percentage differences in Table 13. It has been observed[20] that 20% cold work by hydrostatic extrusion raised the yield and ultimate strengths at 1200°F by 37% and 20%, respectively, for schedule A6 (B&G Schedule A), and by 44% and 16% respectively, for schedule C7 (B&G Schedule B). The magnitudes are appreciably lower than the corresponding average increases of about 65% and 37% obtained in the present investigation. This apparent discrepancy will be resolved later in this section.

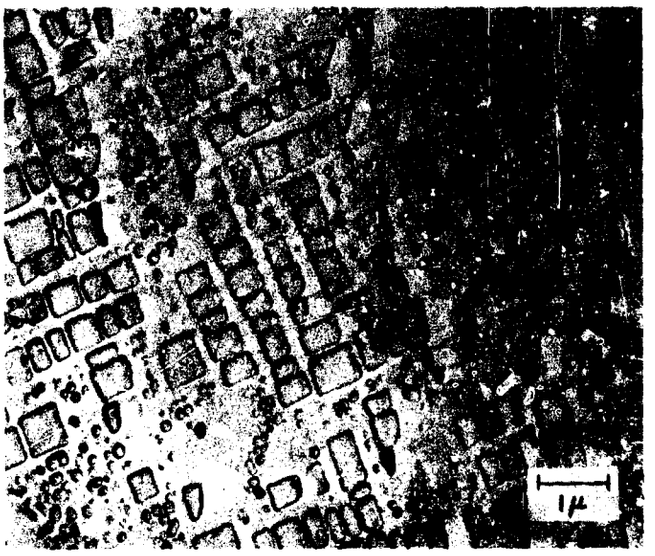

a. Solution Treated, γ' and Carbide Aged

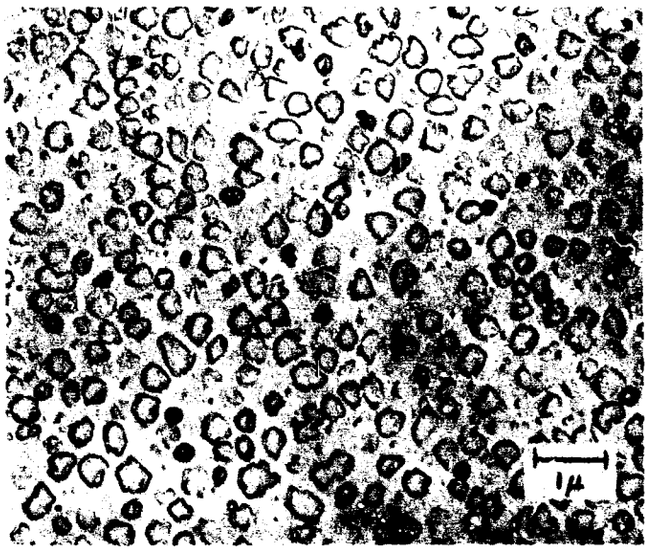

b. Solution Treated, Shocked to 527 kbar, γ' and Carbide Aged

Figure 11. Influence of Shock-Aging on Gamma Prime Morphology and Distribution in Udimet 700.

Table 12. Tensile Properties of Udimet 700 at 1200°F Following Thermal Processing (STA), Conventional TMP (19.1% Reduction), and Shock TMP (527 kbar). Mean Values are Underlined

TMP Schedule	0.2% YS (ksi)	UTS (ksi)	Elong. (Percent)	R.A. (Percent)
STA	95.9	128.7	3.8	7.0
	98.1	125.3	3.2	5.8
	97.0	127.0	3.5	6.4
AR6	159.4	171.3	1.5	6.7
	160.4	179.4	2.4	4.3
	159.9	175.3	1.9	5.5
AS6	146.2	177.5	14.5	23.5
	141.3	162.5	9.1	28.8
	143.8	170.0	11.8	26.2
BR7	163.5	191.8	5.1	6.9
	163.1	190.5	5.1	11.4
	163.3	191.1	5.1	9.1
BS7	150.4	168.9	14.0	32.8
	143.2	171.8	11.3	33.1
	146.8	170.4	12.7	33.0
CR7	161.1	175.6	1.6	5.4
	157.3	167.6	3.0	8.6
	159.2	171.6	2.3	7.0
CS7	145.6	175.3	14.1	27.5
	143.0	166.9	10.3	33.5
	144.3	171.1	12.2	30.5
Nominal	124	180	16	20

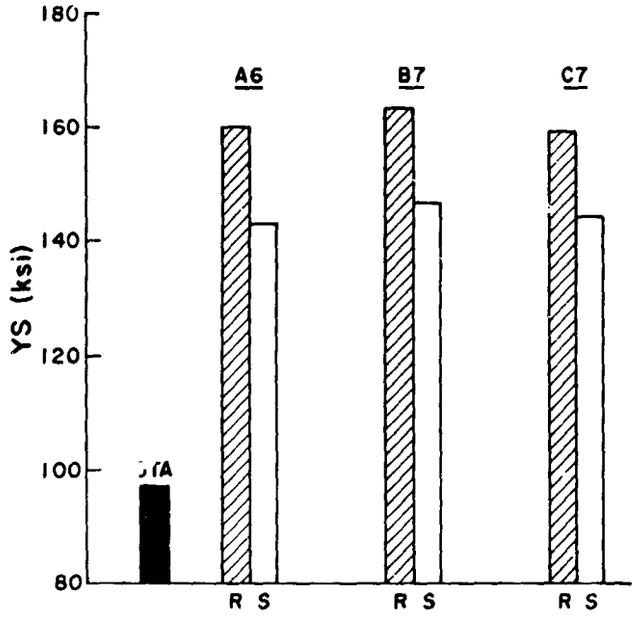

(a) Yield Strength (0.2% offset)

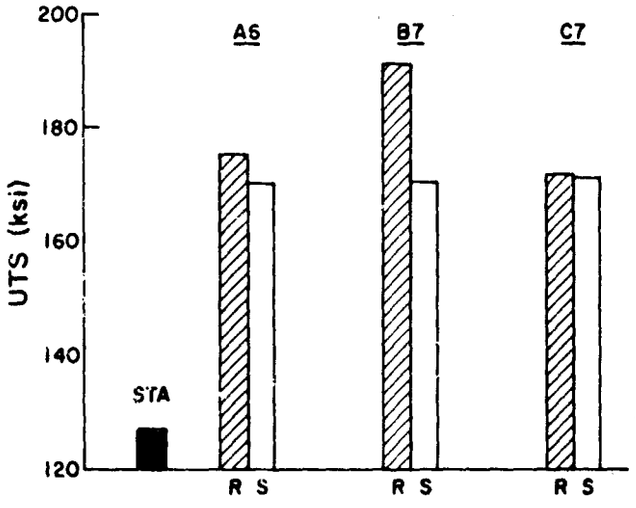

(b) Ultimate Tensile Strength

Figure 12. Tensile Strengths of Udimet 700 at 1200°F Following Thermal Processing (STA), Conventional TMP by Cold Rolling (R; 19.1% Reduction), and Shock TMP (S; 527 kbar)

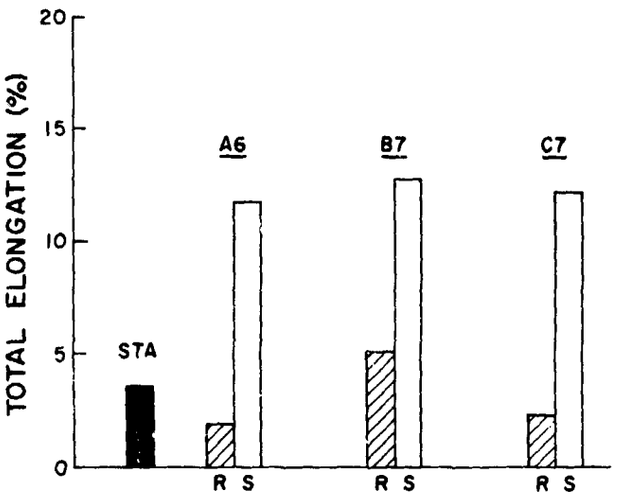

(a) Total Elongation

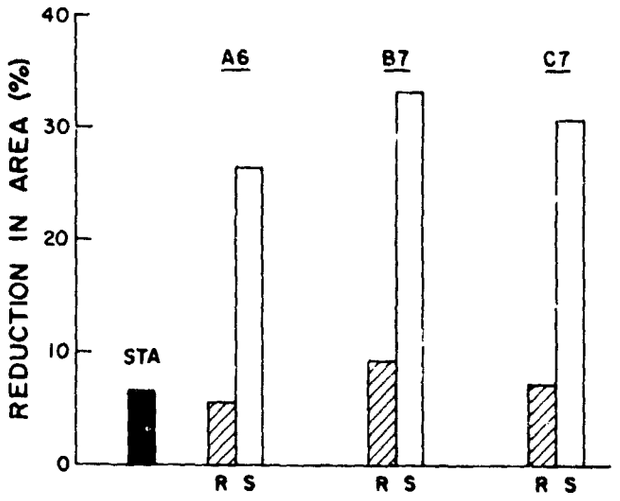

(b) Reduction in Area to Fracture

Figure 13. Tensile Ductilities of Udimet 700 at 1200°F Following Thermal Processing (STA), Conventional TMP by Cold Rolling (R; 19.1% Reduction), and Shock TMP (S; 527 kbar)

Table 13. Percentage Change in 1200°F Tensile Properties of Udimet 700 Due to Shock or Conventional TMP Relative To Full Heat Treatment

Comparison		Schedule	0.2% YS	UTS	Elong.	R.A.
$\frac{\text{R-STA}}{\text{STA}}$	(%)	A6	+65	+38	- 46	- 14
		B7	+68	+50	+ 46	+ 42
		C7	+64	+35	- 34	+ 9
$\frac{\text{S-STA}}{\text{STA}}$	(%)	A6	+48	+34	+237	+309
		B7	+51	+34	+263	+416
		C7	+49	+35	+249	+377
$\frac{\text{S-R}}{\text{R}}$	(%)	A6	-10	- 3	+521	+376
		B7	-10	-11	+149	+263
		C7	- 9	0	+450	+336

An interpretation of TMP strengthening, either by cold rolling or shock loading, is impossible at this time. Nevertheless, some comments on this subject are in order. As suggested in Section 5.1, only about one-half of the strengthening is thought to be due directly to the interaction of dislocations with the prior deformation substructure. In addition, the γ' particle size in the STA condition is about twice that in material processed according to schedule A6 since the γ' aging step is absent in the latter instance. Thus, one could reconcile part of the strength difference between STA and A6 in terms of the γ' size difference. However, when one considers the fact that the size of the γ' is approximately the same after STA, B7, and C7 processing, while the strengths of A6, B7, and C7 exceed that of STA by nearly the same amount, then this explanation seems untenable. Tentatively, this investigator contends that the TMP strengthening is attributable to the presence of a deformation substructure which is equilibrated to some extent by thermal recovery at the lower aging temperatures and further stabilized by the nucleation of a fine $M_{23}C_6$ carbide on the dislocations of the recovered substructure. That this carbide can and does nucleate on dislocations in nickel-base alloys has been shown by other investigators[23-25]. Conceivably, other factors, such as a variation of coherency strain due to the presence of the substructure, or the substructure hardening of the γ' precipitate itself, could provide some contribution to the strengthening but the author is unaware of any supporting evidence in this regard. Strengthening mechanisms such as

solid solution hardening, anti-phase boundary energy, and stacking-fault energy are not expected to be sensitive to prior work.

For equivalent effective strains, using transient shock strain as a comparison, shock TMP generally resulted in somewhat less (0 to 11%) strength improvement over thermally processing than conventional TMP. That a small difference exists, regardless of sign, is not considered to be particularly significant at this time. In a sense, the utilization of strain itself, and moreover, an equivalent generalized strain, in the assessment of the effects of one type of deformation process relative to another is rather arbitrary. Differing states of stress and strain could have a bearing on the results. Not until substructure information becomes available can a rigorous evaluation be made of the relative contributions of strain rate and other factors to strengthening. The most important point is that a reduction in thickness of nearly 20% by cold rolling will produce roughly the same strengthening effect as a 527 kbar compressive shock. It is obvious that this would not be true if the rolling strain were decreased by an order of magnitude to about 2%, a value which is then equivalent to the residual shock strain -- a parameter that describes the actual dimensional change undergone during shock wave propagation. In this case, then, the magnitude of the shock-age strengthening relative to that achievable through techniques involving quasi-static deformation can be taken as being very nearly equal to the change in strength from the thermally processed control material. On the residual strain basis, therefore, shock TMP would appear to have considerable potential for applications where dimensional changes have to be kept to a minimum.

One would anticipate that an increase in strength due to TMP would be accompanied by a decrease in tensile ductility.[19, 20] Indeed, as seen from Table 13, this was true for conventional TMP except for schedule B7 which yielded an increase in ductility of over 40%. Alternatively, shock TMP led to a rise in total elongation of about 250% for all three schedules, compared with normally heat treated control material. Correspondingly, the areal reduction exhibited a 4- to 5-fold increase.

It seems reasonable to expect that microscopic flaws preexist in the Udimet 700 sheet used in this study. For example, a number of the massive precipitates appear to be cracked, presumably as a result of the deformation required to achieve the 95-mil thickness.

Consequently, the major contribution to the enhanced ductility probably derives from the increased difficulty of crack propagation. Whether the cracks are relaxed by preferential slip due to the presence of a high density of short mobile dislocation segments, or whether the cracks are blunted by, say, a fine dispersion of matrix $M_{23}C_6$ due to nucleation on dislocations, is open to speculation. A major factor in the large difference in ductility between conventional and shock TMP could be the condition of the MC and M_3B_2 precipitates. As can be seen in Figure 14, those in the former material exhibited severe cracking while in the latter, they remained relatively intact. Such deterioration was prevalent in all rolled material and absent in all shocked samples. (Cracks are present in the large precipitates of the sample in Figure 10(a) but are not resolved.) This illustrates another advantage of shock TMP, An enhancement in fracture toughness induced by shock-aging is also suggested.

The preceding observations and conclusions, including the stress-rupture behavior presented in the next section, pertain to a particular material, i.e., Udimet 700 sheet received from the Stellite Division, and to a particular heat treatment with temperatures and times the same as those suggested as standard by Special Metals, Inc.[36] Thus, the findings are self-consistent. Attention now is drawn to the fact that the 1200°F tensile properties of solution treated and aged Udimet 700 sheet do not conform to those quoted as nominal by Special Metals, Inc.[36] This is evident from Table 12. The reasons for this discrepancy are not fully understood. The heat treatment schedule given by Kelley[35] for 30-mil sheet involves reductions in solutionizing time and temperature and γ' aging temperature. A rapid air cool was specifically included as part of the solution treatment. Since the composition of the 95-mil sheet fell within nominal limits and since it was found initially that a 2150°F annual for 4 hours will dissolve the γ', there seemed to be little reason to alter the standard heat treatment, at least not until the conduct of optimization studies.

Since it was felt that the strength and ductility inadequacies were related to the heat treatment, the effect of a modification on tensile properties was investigated. The parameters were changed from the standard values given in Section 4.1 to 2150°F/30 min. and 1950°F/4 hr., with the carbide and final ages remaining unchanged. Also, the material was oil quenched from 2150°F. As predicted from the composition, solutionizing at 2050°F for 30 min., conditions suggested by Kelley for 30-mil sheet, was found to be insufficient to dissolve the γ' completely.

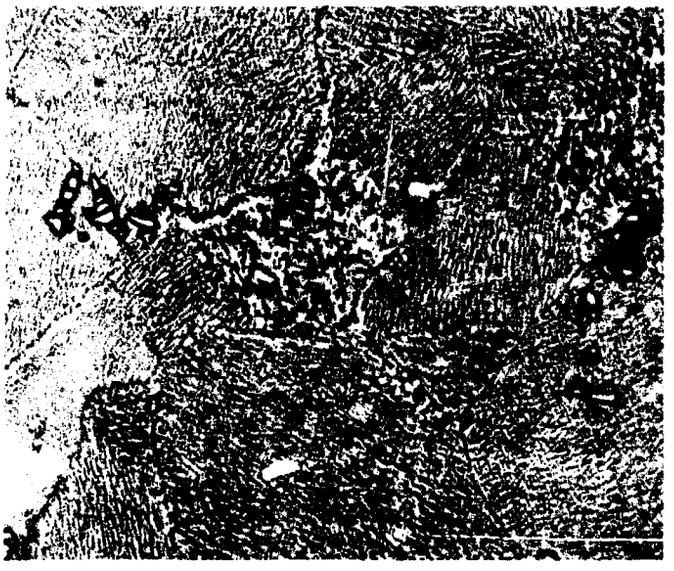

a. Cold Rolled to 19. 1% Reduction in Thickness: 500X

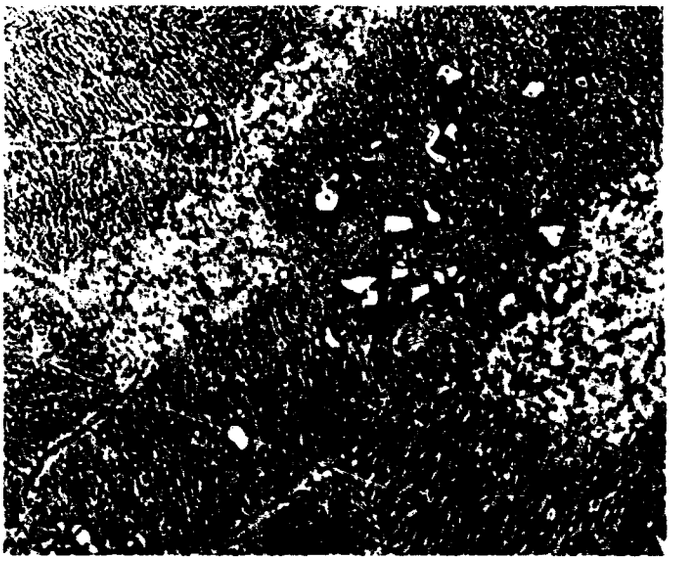

b. Shock Loaded to 527 kbar; 500X

Figure 14. Condition of Massive Precipitates in Udimet 700; History C.

The tensile properties at 1200°F are given in Table 14 for the modified A6 schedule (MA6) and the thermally processed control material (MSTA). The strength of the latter comes within about 4% of nominal values but the ductility is still low by an appreciable margin. With the modified heat treatment, the average increase in yield stress was about 50 ksi instead of 55 ksi typical of the standard schedule, and in ultimate strength, 30 ksi instead of 45 ksi. However, it should be noted that the yield and ultimate strengths which were used for comparison, were also higher by about 23 and 47 ksi. Thus, when alloy strengthening is more pronounced, the effect of TMP tends to be lower. This is in keeping with the suggestion that part of the strength enhancement resides directly in substructure hardening; this mechanism plays a smaller role the higher is the basic strength. Nevertheless, other substructure-related effects appear to be retained.

Table 14. Tensile Properties of Udimet 700 at 1200°F Following Thermal Processing (MSTA), Conventional TMP (19.1% Reduction), and Shock TMP (527 kbar). Modified Heat Treatment. Mean Values are Underlined

TMP Schedule	0.2% YS (ksi)	UTS (ksi)	Elong. (Percent)	R.A. (Percent)
	119.8	174.4	6.3	12.2
MSTA	120.4	173.2	5.9	10.2
	120.1	173.8	6.1	11.2
	175.9	208.2	5.6	9.9
MAR6	177.1	203.1	5.7	9.4
	176.5	205.6	5.7	9.6
	176.0	204.5	4.8	8.6
MAS6	169.2	201.2	7.6	10.2
	173.1	202.9	6.2	9.4
	123.9	185.5	14.2	16.5
MSTA-2	121.3	176.3	6.3	10.7
	122.6	180.9	10.2	13.6
Nominal	124	180	16	20

The percentage strength differences listed in Table 15 for the modified TMP schedules are in good agreement with the strength

increases of 37 and 20% for yield and ultimate strengths, respectively, obtained by Blankenship and Gyorgak[20]. They reported 1200°F yield and ultimate values of 179 ksi and 219 ksi, respectively, for TMP schedule A with 20% strain by hydrostatic extrusion.

Table 15. Percentage Change in 1200°F Tensile Properties of Udimet 700 Due to Shock or Conventional TMP Relative to Full Modified Heat Treatment

Comparison	0.2% YS	UTS	Elong.	R.A.
$\frac{\text{R-MSTA}}{\text{MSTA}}$ (%)	+47	+18	-7	-14
$\frac{\text{S-MSTA}}{\text{MSTA}}$ (%)	+36	+17	+1	-16
$\frac{\text{S - R}}{\text{R}}$ (%)	- 2	- 1	+9	- 2

Conventional TMP, using the altered heat treatment schedule, produced a small decrease in the ductility parameters. Whereas Blankenship and Gyorgak[20] observed a 65% decrease in overall ductility, the final values were still higher than those measured in the present study. Changes similar to those resulting from the modified conventional TMP schedule were measured after shock TMP which also incorporated the modified solution treatment, although the total elongation was marginally better than after thermal processing. At this stage of the investigation, any interpretation of the relative effect of the standard and modified shock-aging schedules on terminal ductility is subject to the results of more detailed studies.

The above work has disclosed, firstly, that in some circumstances TMP can serve as a substitute for heat treatment when the conditions are removed from those necessary to develop optimum properties, and secondly, that TMP can lead to appreciable strength improvements even when the thermal treatment parameters used would ordinarily yield optimum properties.

The designation MSTA-2 in Table 14 corresponds to a second heat of Udimet 700 from Stellite.

5.4 Stress-Rupture Behavior

The stress-rupture life and ductility were measured at a temperature of 1200°F under a constant load corresponding to an initial stress of 120,000 psi. The results of the application of schedules A6, B7, and C7, with a shock pressure of 527 kbar or rolling reduction of 19.1%, were compared with fully heat treated material (standard heat treatment).

Only one specimen has been tested for each condition thus far so that the evaluation should not be considered complete. Nevertheless, there seems to be little doubt from the data in Table 16 and the bar graphs of Figure 15 that TMP has introduced a marked improvement in rupture life. Moreover, shock-aging holds an advantage over conventional TMP for schedules A6 and C7, while the difference is reversed for schedule B7. The 50-fold increase in rupture life with schedule AS6 compares more than favorably with the 9-fold increase obtained by Blankenship and Gyorgak[20] for the same schedule but with 20% hydrostatic extrusion. Similarly, the 15-fold increase with schedule CS7 is greater than the 2-fold increase obtained by the above investigators using the same schedule but again, with 20% extrusion. However, as with the tensile data, it must be pointed out the base-line STA value of 5.1 hours is much lower that the STA life of 429 hours measured by Blankenship and Gyorgak[20]. Of the three schedules examined, A6 appears to be the most promising, in agreement with previous work[20].

Table 16. Stress-Rupture Properties of Udimet 700 at 1200°F and 120,000 psi Following Thermal Processing (STA), Conventional TMP (19.1% Reduction), and Shock TMP (527 kbar)

TMP Schedule	Rupture Life (Hour)	Elongation (Percent)
STA	5.1	2.3
AR6	195.4	1.9
AS6	243.7	5.7
BR7	146.9	0.5
BS7	45.1	0 8
CR7	45.2	1.6
CS7	73.1	1.6

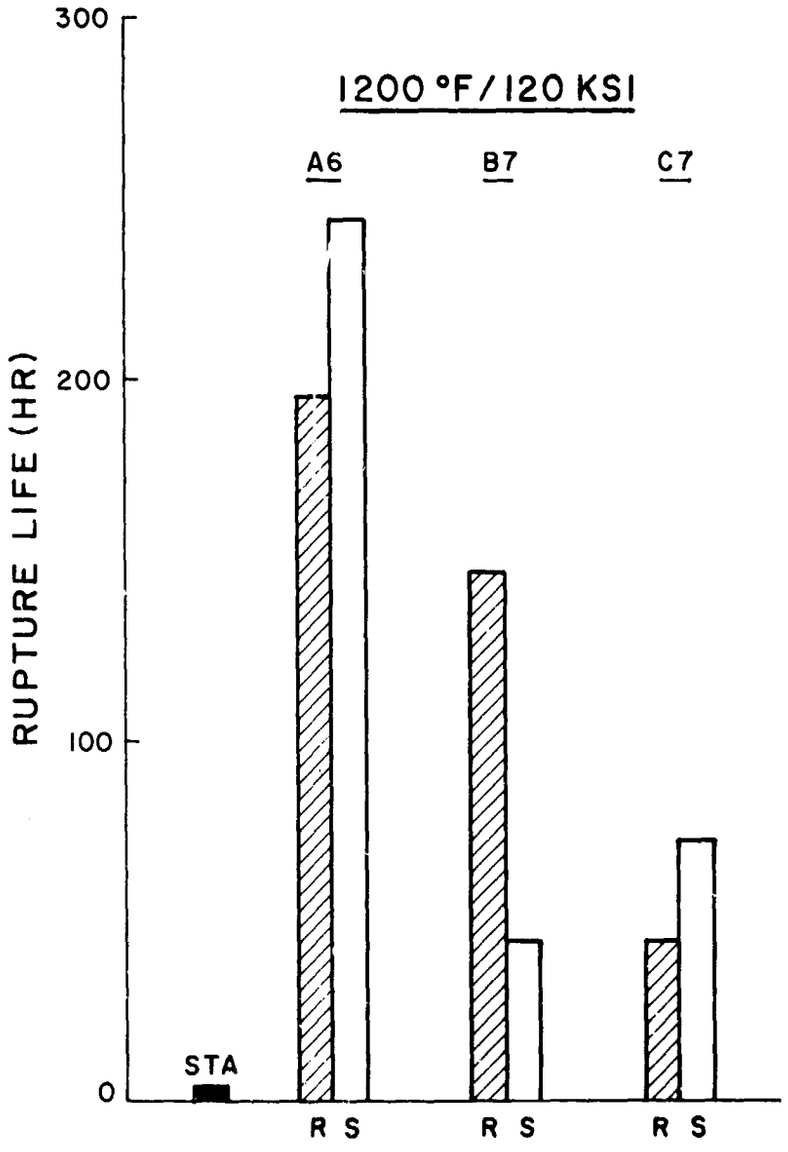

Figure 15. Stress-Rupture Life of Udimet 700 Following Thermal Processing (STA), Conventional TMP by Cold Rolling (R; 19.1% Reduction), and Shock TMP (S; 527 kbar)

To the authors knowledge, only two investigations have dealt with the creep behavior of shocked nickel-base alloys. In both studies, the material was tested in the prestrained condition where aging, when applicable, preceded shock deformation; neither involved aging after shocking. Leverant and Kear[49] found that the dislocation substructure generated by the propagation of a 250 kbar shock wave through a Mar-M200 single crystal was sufficient to eliminate the incubation period for creep. This result, although interesting, has no direct bearing on the present work. Studies by Harrigan[50] on a solid solution alloy (Ni-20%Cr) and a γ' precipitation-hardened alloy (Ni-18%Cr-4%Al) showed that shock loading to 70 kbar reduced the creep rate of the former material, but the effects on the latter tended to be deleterious. The Udimet 700 examined herein also contained a γ' precipitate when shock loaded. Although the particle size varied, this was true irrespective of history. Thus, Harrigan's results suggest that the as-shocked conditions AS, BS, and CS might exhibit rupture properties which are inferior to that of the fully heat treated material. On the other hand, present data indicate that if Harrigan had further aged his Ni-Cr-Al alloy after shock loading, he would not only have eliminated the detrimental effects observed but effected substantial improvements in creep properties.

A study of the factors responsible for the enhancement of stress-rupture life by TMP and the effect of TMP on overall creep behavior is planned.

6. SUMMARY AND CONCLUSIONS

The results of this investigation and the conclusions drawn therefrom may be summarized as follows.

1. Udimet 700 nickel-base superalloy can be successfully compression shock loaded to 527 kbar, even when almost fully hardened, without spallation and fracture; the residual strain corresponding to this shock pressure is only about 2% with the type of loading system used.

2. A Hugoniot curve for a complex alloy can be constructed from the Hugoniot data for the individual alloying constituents by the summation of their fractional contributions according to atomic composition; the shock velocity versus particle velocity relation for Stellite Udimet 700 sheet is

$$U = 4.913 + 1.316u \quad \text{mm}/\mu\text{sec}.$$

3. Solution treated, or partially aged Udimet 700 exhibits the expected strain hardening as a result of cold rolling or shock loading, an effect which increases with increasing strain or shock pressure. The appearance of slip bands in the former and almost complete absence in the latter suggests that the deformation substructure is on a much finer scale in the shocked material.

4 This strengthening effect is retained during subsequent aging irrespective of whether the Udimet 700 is in the solution treated or partially aged condition prior to deformation; also, the pre-strain dependence of the strengthening remains positive.

5. The room temperature strengthening of Udimet 700 (as measured by hardness) due to shock TMP is normally less than that due to conventional TMP for a rolling reduction equivalent to the transient shock strain; on a residual shock strain basis, however, shock TMP produces a substantial increase in strength over conventional TMP for high shock pressures.

6. Both conventional and shock TMP at the 20% strain level generate a substantial increase in the 1200°F yield and ultimate strengths of Udimet 700.

7. When the thermal treatment parameters of the TMP schedules are such that tensile strengths produced by thermal processing alone are below optimum values, the conventional TMP reduces tensile ductilities at 1200°F; conversely, shock-aging leads to ductility increases ranging from about 200 to over 400%. If the heat treatment variables are modified to yield nearly nominal strengths by thermal processing, then relatively little change in 1200°F tensile ductility appears to accompany the strength increases due to conventional or shock TMP.

8. Both conventional and shock TMP at the 20% strain level produce appreciable increases in the 1200°F/120 ksi stress-rupture life of Udimet 700. For two out of three schedules examined, shock TMP proved superior to conventional TMP. For example, schedule AS6 (2150°F/4hr. + 527 kbar shock + 1550°F/24 hr. + 1400°F/16 hr.) resulted in almost a 50-fold improvement in life, from 5 hour for thermally processed material to 244 hour for shock-aged specimens.

9. Cold working by rolling fractures the massive precipitates (MC and M_3B_2) present in Udimet 700 while compression shock loading results in little detectable deterioration. This is thought to be responsible, at least in part, for the large discrepancy in ductility observed between conventionally and shock processed material.

10. Cold working by rolling in the solution treated condition results in the formation of a cellular precipitate in Udimet 700 during subsequent aging at 1975°F for 4 hour; this kind of microstructural instability was not detected when shock loaded material was similarly aged.

11. The aging of Udimet 700 at 1975°F for 4 hour after deformation by rolling or shocking in the solution treated condition tends to randomize the distribution of matrix γ' and to change its shape from the common cuboidal form to a more spheroidal geometry.

12. An analysis of the data suggests that one can tentatively attribute about 50% of the strengthening of Udimet 700 by TMP directly to the deformation substructure. The remainder is postulated to be due to the presence of a fine $M_{23}C_6$ precipitate nucleated at matrix dislocations.

13. When the effects on mechanical properties and microstructure, and the small dimensional changes incurred during shock loading are taken into consideration, it can be concluded that thermo-mechanical processing utilizing shock deformation is superior to conventional TMP. Due to the small residual shock strains, one particular advantage of such a shock-aging process is its potential for strengthening normally solidified and unidirectionally solidified castings, powder compacts, forgings, etc., when little dimensional change can be tolerated before final sizing is effected.

7. AREAS FOR FURTHER STUDY

The potential of thermomechanically processing Udimet 700 by utilizing shock deformation as the mechanical working step has been clearly demonstrated. The next phase of the study which is presently underway includes the optimization of TMP parameters, the determination of the maximum temperature at which TMP strengthening can be considered effective, the assessment of microstructural stability, an evaluation of properties other than tensile and creep which could benefit from shock TMP, and the establishment of the mechanisms which contribute to the improvement of properties. This last factor is extremely important to the prediction of which alloys would benefit most from TMP, and shock TMP in particular.

It is known that the low coherency strain associated with γ' in Udimet 700 does not favor its nucleation at dislocations. Accordingly, future plans include the investigation of shock aging of an alloy containing a Ni_3Nb precipitate which has a greater mismatch with the matrix and has been observed to form on line defects. Inconel 718 was selected for this purpose.

In addition, plans are being formulated to examine the application of shock TMP to other alloy systems.

ACKNOWLEDGEMENTS

The author is indebted to the Naval Air Systems Command for the opportunity to conduct this research, and to Mr. Irving Machlin for helpful suggestions. The technical assistance of R. L. Clark and D. L. Stratford are gratefully acknowledged. The author also wishes to express his appreciation to L. F. Trueb, R. H. Wittman, and C. P. Blankenship for fruitful discussions. Special thanks are extended to the Stellite Division of Cabot Corporation and E. W. Kelley for the provision of the Udimet 700 sheet.

REFERENCES

1. Sims, C. T., "Nickel Alloys - The Heart of the Gas Turbine Engines," ASME Paper No. 70-GT-24, presented at the ASME Gas Turbine Conference, Brussels, Belgium, May (1970).

2. Allen, M. M., Athey, R. L. and Moore, J. B., "Application of Powder Metallurgy to Superalloy Forgings," Metals Eng. Quart. 10, No. 1, February 20-30 (1970).

3. Athey, R. L. and Moore, J. B., "Development of IN100 Powder Metallurgy Disks for Advanced Jet Engine Application," private communication, Pratt and Whitney Aircraft, West Palm Beach, Florida (1971).

4. Freche, J. C., Waters, W. J. and Ashbrook, R. L., "Evaluation of Two Nickel-Base Alloys. Alloy 713C and NASA TAZ-8A, Produced by Extrusion of Prealloyed Powder," Metals Eng. Quart. 10, No. 2, May, 58-9 (1970).

5. Friedman, G. and Kosinski, E., "High-Performance Material from a Hot-Worked Superalloy Powder," Metals Eng. Quart. 11, No. 1, February, 48-50 (1971).

6. Piearcey, B. J. and VerSnyder, F. L., "A New Development in Gas Turbine Materials: The Properties and Characteristics of PWA 664," J. Aircraft 3, 390-7 (1966).

7. Piearcey, B. J. and VerSnyder, F. L., "Monocrystaloys: A New Concept in Gas Turbine Materials; The Properties and Characteristics of PWA 1409," Pratt and Whitney Aircraft, Report No. 66-007, February 2 (1966).

8. Kear, B. H. and Piearcey, B. J., "Tensile and Creep Properties of Single Crystals of the Nickel-Base Superalloy Mar-M200," Trans. TMS-AIME 239, 1209-15 (1967).

9. E. R. Thompson and F. D. Lemkey, "Structure and Properties of Ni_3Al (γ') Eutectic Alloys Produced by Unidirectional Solidification," Trans. ASM 62, 140-54 (1969).

10. "Inconel Alloy 718," Huntington Alloy Products Division, International Nickel Co., Inc., Huntington, West Virginia (1968).

11. "Engineering Properties of Monel Alloy K-500," Tech. Bulletin T-9, Huntington Alloy Products Division, International Nickel Co., Inc., Huntington, West Virginia (1965).

12. Slunder, C. J. and Hall, A. M., "Thermal and Mechanical Treatments for Nickel and Selected Nickel-Base Alloys and Their Effect on Mechanical Properties," Battelle Memorial Institute, NASA TMX-53443, April (1966); AD 633 040.

13. Hotzler, R. K., Maciag, J., Fischer, G. J. and Troc, E., "Thermomechanical Working of Astrology," Met. Trans. 1, 963-7 (1970).

14. Dunleavy, J. G. and Spretnak, J. W., "Soviet Technology on Thermal-Mechanical Treatment of Metals," Battelle Memorial Institute, DMIC Memo. 244, November (1969).

15. Sokolkov, Ye. N., Gaydukov, M. G. and Petrova, S. N., "Features of the Initial Stage of Creep in an Alloy of the Nimonic Type After High Temperature Thermomechanical Treatment," Fiz. Met. i Metallov. 19, 91-4 (1965).

16. Henning, H. J., "Applications and Potential of Thermomechanical Treatment," Battelle Memorial Institute, DMIC Memo. 251, November (1970).

17. Wukusick, C. S. and Smashey, R. W., "Ultra High-Strength Superalloys," General Electric Co., Technical Report AFML-TR-68-214, October (1968); AD 843 981.

18. Kear, B. H., Oklak, J. M. and Owczarski, W. A., "Thermomechanical Processing of the Nickel-Base Alloy U-700," paper presented at WESTEC Conference, Los Angeles, California, March (1971).

19. Blankenship, C. P., "Thermomechanical Processing of the Nickel-Base Alloy U-700," presented at the Aerospace Structural Materials Conference, Lewis Research Center, NASA, Paper No. 6, November 18-19 (1969); Conf. Proc., NASA Report SP-227, pp. 91-100 (1970).

20. Blankenship, C. P. and Gyorgak, C. A., "Thermomechanical Processing of the Nickel-Base Alloy U-700," NASA TN D-6418, September (1971).

21. Nutting, J., "The Influence of Plastic Strain Upon the Aging Characteristics of Alloys," Met. Trans. 2, 45-51 (1971).

22. Phillips, V. A., "A Metallographic Study of Precipitation in a Ni-12.7 at. % Al Alloy," Acta Met. 14, 1533-47 (1966).

23. Kotval, P. S , Carbide Precipitation on Imperfections in Superalloy Matrices," Trans. TMS-AIME 242, 1651-6 (1968).

24. Kotval, P. S., "The Microstructure of Superalloys," Metallography 1, 251-85 (1969).

25. Rowe, G. M., Rand, W. H and Kear, B. H., "On the Mechanism of Formation of Stacking Faults in Aged Nickel-Base Alloys," Proc. 26th Annual EMSA Meeting, 262-3 (1968).

26. Holtzman, A. H. and Cowan, G. R., "The Strengthening of Austenitic Manganese Steel by Plane Shock Waves," Response of Metals to High Velocity Deformation, ed. P. G. Shewmon and V. F. Zackay, Interscience, 447-82 (1961).

27. Dieter, G E., "Hardening Effect Produced with Shock Waves," Strengthening Mechanisms i. Solids, American Society for Metals, 279-340 (1962).

28. Nolder, R. L. and Thomas, G., "The Substructure of Plastically Deformed Nickel," Acta Met. 12, 227-40 (1964).

29. Mahajan, S., "Metallurgical Effects of Planar Shock Waves in Metals and Alloys," phys. stat. sol. (a) 2, 187-201 (1970).

30. Weertman, J., "High Velocity Dislocations," source cited in Ref. 26, 205-47.

31. Kressel, H. and Brown, N., "Lattice Defects in Shock-Deformed and Cold-Worked Nickel," J. Appl. Phys. 38, 1618-25 (1967).

32. Rose, M. F. and Berger, T. L., "Shock Deformation of Polycrystalline Aluminum," Phil. Mag. 17, 1121-33 (1968).

33. Christou, A., "Point Defect Recovery of Shock Deformed Iron Alloys," Scripta Met. 5, 749-52 (1971).

34. Kelley, E. W., "Manufacturing Process for Improved High-Strength Superalloy Sheet," Union Carbide Corp., Technical Report AFML-TR-69-114, June (1969).

35. Kelley, E. W., "A Manufacturing Process For U-700 Alloy Thin Gage Sheet," Met. Eng. Quart. 11, No. 1, February, 10-16 (1971)

36. "Alloy Performance Data, Udimet 700," Special Metals, Inc., New Hartford, New York.

37. Boesch, W. J. and Canada, H. B., "Phases Present in the Wrought Superalloy Udimet 700," J. Metals 20, No. 4, April, 46-50 (1968).

38. Wittman, R. H., Denver Research Institute, University of Denver, Denver, Colorado 80210, private communication (1971).

39. Rice, M. H., McQueen, R. G. and Walsh, J. M., "Compression of Solids by Strong Shock Waves," Solid State Physics 6, 1-63 (1958).

40. Duvall, G. E., "Some Properties and Applications of Shock Waves," source cited in Ref. 26, 165-203.

41. Skidmore, I. C. and Morris, E., Thermodynamics of Nuclear Materials, International Atomic Energy Agency, Vienna, 173 (1962).

42. Doran, D. G., "Hugoniot Equation of State of Pyrolytic Graphite to 300 Kbars," J. Appl. Phys. 34, 844-50 (1963).

43. Walsh, J. M., Rice, M. H., McQueen, R. G. and Yarger, F. L., "Shock-Wave Compressions of Twenty-Seven Metals. Equation of State of Metals," Phys. Rev. 108, 196-216 (1957).

44. Kriege, O. W. and Baris, J. M., "The Chemical Partitioning of Elements in Gamma Prime Separated from Precipitation-Hardened, High-Temperature Nickel-Base Alloys," Trans. ASM 62, 195-200 (1969).

45. Lubahn, J. D. and Felgar, R. F., Plasticity and Creep of Metals, Wiley, 286 (1961).

46. Murr, L. E., Vydyanath, H R. and Foltz, J. V., "Comparison of the Substructures and Properties of Nickel, TD-Ni, Chromel-A, Inconel 600, and TD-NiCr Following Explosive-Shock Deformation," Met. Trans. 1, 3215-23 (1970).

47 Murr, L. E. and Vydyanath, H. R., "Thermal Recovery of Explosive Shock-Loaded Ni, TD-Ni, Chromel-A, Inconel 600, and TD-NiCr," Acta Met. 18, 1047-52 (1970).

48. Oblak, J. M. and Owczarski, W. A., "Cellular Recrystallization in a Nickel-Base Superalloy," Trans. TMS IME 242, 1563-8 (1968).

49. Leverant, G. R. and Kear, B. H., "The Mechanism of Creep in Gamma Prime Precipitation-Hardened Nickel-Base Alloys at Intermediate Temperatures," Met. Trans. 1, 491-8 (1970).

50. Harrigan, W. C. Jr., "A Study of the Effects of Shock Loading and Cold Rolling on High Temperature Creep Properties of Metals and Alloys," Stanford University, Report No. SU-DMS-71-T-52, March (1971).